Journal of Organometallic Chemistry, 394 (1990) 385–415
Elsevier Sequoia S.A., Lausanne
JOM 20850

Benzyne complexes of ruthenium: models for dissociative chemisorption of benzene on a metal surface. Crystal structures of $[Ru_4(CO)_{10}(\mu\text{-}CO)(\mu_4\text{-}PR)(\mu_4\text{-}\eta^4\text{-}C_6H_4)]$ (R = Ph and CH_2NPh_2), $[Ru_5(CO)_{13}(\mu_4\text{-}PPh)(\mu_5\text{-}\eta^6\text{-}C_6H_4)]$ and $[Ru_6(CO)_{12}(\mu_4\text{-}PMe)_2(\mu_3\text{-}\eta^2\text{-}C_6H_4)_2]$ *

Selby A.R. Knox, Brian R. Lloyd, David A.V. Morton, Sara M. Nicholls, A. Guy Orpen, Josep M. Viñas, Martin Weber and Geoffrey K. Williams

Department of Inorganic Chemistry, The University, Bristol BS8 1TS (U.K.)

(Received February 16th, 1990)

Abstract

Heating a solution of $[Ru_3(CO)_{11}(PPh_3)]$ in toluene gives the μ_3-, μ_4- and μ_5-benzyne complexes $[Ru_3(CO)_7(\mu\text{-}PPh_2)_2(\mu_3\text{-}\eta^2\text{-}C_6H_4)]$ (**1a**) (33%), $[Ru_4(CO)_{10}(\mu\text{-}CO)(\mu_4\text{-}PPh)(\mu_4\text{-}\eta^4\text{-}C_6H_4)]$ (**2a**) (50%) and $[Ru_5(CO)_{13}(\mu_4\text{-}PPh)(\mu_5\text{-}\eta^6\text{-}C_6H_4)]$ (**3a**) (7%), respectively. The structures of **2a** and **3a** have been established by X-ray diffraction, revealing that the benzyne in each case is bound to a square of ruthenium atoms by C-Ru σ-bonds to two adjacent rutheniums, and by η^2-interactions to the other two atoms of the Ru_4 square. In **3a** there is also η^2-co-ordination to a third ruthenium atom, so that there is η^6-co-ordination overall. The five metal atoms of **3a** are arranged like a step site on a metal (111) surface and the complex can be viewed as a model for the aftermath of benzene C–H activation on such a surface. The thermolysis of $[Ru_3(CO)_{11}(PPh_2CH_2NPh_2)]$ gives the μ_4-PCH_2NPh_2 analogue **2b** of **2a**, while from $[Ru_3(CO)_{11}(PPh_2Me)]$ the new cluster $[Ru_6(CO)_{12}(\mu_4\text{-}PMe)_2(\mu_3\text{-}\eta^2\text{-}C_6H_4)_2]$ (**11**) is isolated in 11% yield. The structures of **2b** and of **11** have been determined by X-ray diffraction; **11** contains two μ_3-benzyne ligands bound to triruthenium faces of an Ru_6P_2 cluster. Thermolysis of the tritolylphosphine complexes $[Ru_3(CO)_{11}(PAr_3)]$(Ar = C_6H_4-*m*-Me or C_6H_4-*p*-Me) affords only analogues of **1** and **2**, containing in each case the μ-C_6H_3-4-Me ligand. Heating $[Ru_3(CO)_{11}(AsPh_3)]$ gives low yields of the arsenic analogues of **2** and **3** in addition to the major product $[Ru_2(CO)_6(\mu\text{-}AsPh_2)_2]$ (65%). The fluxional behaviour of complexes **1** and **2**, involving benzyne rotation on Ru_3 and Ru_4 centres, respectively, is discussed, and pathways for the formation of **1**, **2** and **3** are proposed.

---

* Dedicated to Professor F.G.A. Stone F.R.S. on the occasion of his 65th birthday.

0022-328X/90/$03.50

Introduction

The chemisorption of aromatics on metal surfaces has been the subject of much debate [1], but relatively few examples of polynuclear organometallic molecules that could serve as models have been reported. The most attractive are the benzene complex $[Os_3(CO)_9(\mu_3\text{-}\eta^6\text{-}C_6H_6)]$ [2], and benzyne complexes such as $[Ir_2(CO)_2(\mu\text{-}\eta^2\text{-}C_6H_4)(\eta\text{-}C_5H_5)_2]$ [3], $[Os_3H_2(CO)_9(\mu_3\text{-}\eta^2\text{-}C_6H_4)]$ [4–6], $[M_3(CO)_7(\mu\text{-}ER_2)_2(\mu_3\text{-}\eta^2\text{-}C_6H_4)]$ (E = P or As; M = Ru [7,9] or Os [9–11]), $[Os_3H(CO)_9(\mu\text{-}EMe_2)(\mu_3\text{-}\eta^2\text{-}C_6H_4)]$(E = P or As) [10,11] and $[Os_3(CO)_9(\mu_3\text{-}PR)(\mu_3\text{-}\eta^2\text{-}C_6H_4)]$ [12,13]. In this paper we describe the synthesis and structural characterisation of new complexes in which benzyne is co-ordinated at tetra- and penta-ruthenium centres. The five metal atoms of the latter are in the arrangement of a step site on a metal (111) surface and the complex may be seen as a model for the dissociative chemisorption of benzene on such a surface. A preliminary report of this work has appeared [14].

Results and discussion

Benzyne from phenylphosphines

As part of studies [15–19] on the cleavage of P–C bonds at a polynuclear metal centre the monodentate phosphine complex $[Ru_3(CO)_{11}(Ph_2PCH_2NPh_2)]$ was heated in boiling toluene. Several products were formed in low yield but only one was isolated, as red air-stable crystals. No molecular ion was observed in the mass spectrum, but elemental analyses indicated a tetra-ruthenium complex. Proton and ^{31}P NMR spectra (see Experimental) were also not definitive; the former showed the presence of an AA′BB′ system in the aromatic region at δ 5.46 (m, 2H) and 6.44 (m, 2H), suggesting the presence of an *ortho*-C_6H_4 ring, while the latter revealed only a singlet at 415.0 ppm, characteristic of a multiply bridging phosphinidene ligand. It was evident that the $Ph_2PCH_2NPh_2$ ligand had undergone extensive rearrangement and in order to elucidate its nature the product was subjected to an X-ray diffraction study. This established that that the product of thermolysing $[Ru_3(CO)_{11}(Ph_2PCH_2NPh_2)]$ is the μ_4-benzyne complex $[Ru_4(CO)_{10}(\mu\text{-}CO)(\mu_4\text{-}PCH_2NPh_2)(\mu_4\text{-}\eta^4\text{-}C_6H_4)]$ (**2b**). The molecular structure is shown in Fig. 2 and the results are summarised in Tables 2, 5, 6 and 8. The structure is discussed later in relation to other benzyne complexes.

The formation of (**2b**) involves the transformation of the $Ph_2PCH_2NPh_2$ ligand to μ_4-C_6H_4 and μ_4-PCH_2NPh_2, with the loss of a phenyl group and a phenyl hydrogen, presumably as benzene. The CH_2NPh_2 substituent of the phosphine had played no apparent role in the process, leading us to speculate that thermolysis of $[Ru_3(CO)_{11}(PPh_3)]$ might similarly generate the μ_4-PPh analogue of (**2b**). This proved to be the case, but μ_3- and μ_4-benzyne complexes were also produced.

When $[Ru_3(CO)_{11}(PPh_3)]$ is heated in toluene for 18 h three benzyne complexes are formed: $[Ru_3(CO)_7(\mu\text{-}PPh_2)_2(\mu_3\text{-}\eta^2\text{-}C_6H_4)]$ (**1a**) (33%), $[Ru_4(CO)_{10}(\mu\text{-}CO)(\mu_4\text{-}PPh)(\mu_4\text{-}\eta^4\text{-}C_6H_4)]$ (**2a**) (50%) and $[Ru_5(CO)_{13}(\mu_4\text{-}PPh)(\mu_5\text{-}\eta^6\text{-}C_6H_4)]$ (**3a**) (7%), readily separated by chromatography on alumina. A better yield (60%) of **1a** is obtained when $[Ru_3(CO)_{10}(PPh_3)_2]$ is heated in toluene for 2.5 h, but no **2a** or **3a** are produced under these conditions.

The purple crystalline μ_3-benzyne complex **1a** was earlier obtained [7] in 20–30% yield by heating $[Ru_3(CO)_9(PPh_3)_3]$ in decalin or mesitylene and its structure has

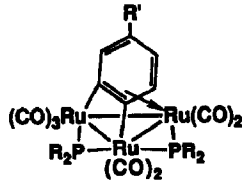

(1a) R = Ph, R' = H
(1b) R = C_6H_3-*m*-Me, R' = Me
(1c) R = C_6H_3-*p*-Me, R' = Me

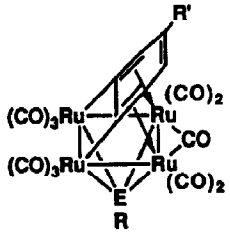

(2a) ER = PPh, R' = H
(2b) ER = PCH_2NPh_2, R' = H
(2c) ER = PC_6H_3-*m*-Me, R' = Me
(2d) ER = PC_6H_3-*p*-Me, R' = Me
(2e) ER = AsPh

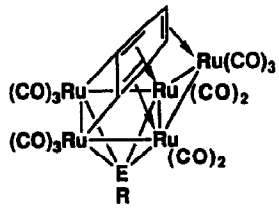

(3a) ER = PPh
(3b) ER = AsPh

been determined by X-ray diffraction to be as shown [8]. The ^{1}H NMR spectrum of **1a** was previously recorded only at room temperature, but it is clear from variable-temperature ^{1}H and ^{31}P NMR studies reported here that the complex is fluxional. Thus, the room-temperature ^{31}P NMR spectrum displays a sharp singlet at 239.6 ppm, which is broadened at $-90\,^\circ$C, indicating the existence of a low energy process which renders the two phosphorus nuclei equivalent on the NMR time scale. This fluxionality is also evident in the ^{1}H NMR spectrum. At $-45\,^\circ$C four signals of equal intensity are seen for the benzyne protons at δ 6.44 (t, J 6 Hz, 1H), 6.54 (t, J 6 Hz, 1H), 6.73 (d, J 7 Hz, 1H), and 7.19 (d, J 7 Hz, 1H) in the expected ABCD pattern. These broaden and coalesce pair-wise on warming until at room temperature two broad signals are observed, which at $50\,^\circ$C sharpen to signals at δ 6.47 (2H) and 6.98 (2H), which are clearly those of an AA'BB' system. These observations are similar to those made for the related μ_3-benzyne complexes $[Os_3(CO)_7(\mu\text{-}EMe_2)_2(\mu_3\text{-}\eta^2\text{-}C_6H_4)]$ (E = P or As), which were explained on the basis of two fluxional processes occurring in concert, namely a "rotation" of the benzyne about the metal triangle and a "flip" which interchanges the two faces of the ligand [10,11]. It therefore seems likely that these same processes are operating for **1a**. From the data for **1a** it is clear that the flip, which averages the phosphorus environments, occurs rapidly even at $-90\,^\circ$C and that the rotation, which causes pair-wise averaging of the benzyne protons, is a much higher energy process. The free energy of activation ΔG^* for the rotation is estimated to be 56 ± 1 kJ mol^{-1} from the coalescence of the proton signals at δ6.73 and 7.19 ($T_c = 292$ K). This compares with $\Delta G^* = 58.0$ kJ mol^{-1} ($T_c = 278$ K) for $[Os_3(CO)_9(\mu\text{-}PMe_2)_2(\mu_3\text{-}\eta^2\text{-}C_6H_4)]$ and 51.3 kJ mol^{-1} ($T_c = 248$ K) for $[Os_3(CO)_9(\mu\text{-}AsMe_2)_2(\mu_3\text{-}\eta^2\text{-}C_6H_4)]$ [10].

Red crystalline **2a** was identified as the μ_4-PPh analogue of **2b** on the basis of its IR and NMR spectra, and unequivocal structural characterisation was achieved by X-ray diffraction. The structure of **2a** is shown in Fig. 1 and the results of the structural study are summarised in Tables 1, 5, 6 and 7. Full discussion of the structure is given later, but it is worth noting here that a complex $[Ru_4(\mu\text{-}H)_2(CO)_{11}(\mu\text{-}PR)(\mu_4\text{-}\eta^2\text{-}C_6H_4)]$ (R = ferrocenyl) (**4**)) with a related μ_4-benzyne ligand has been briefly reported by Cullen et al.; the benzyne is co-ordinated to an Ru_4 square as an η^2-alkyne [20].

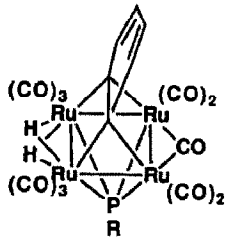

(4) R = $C_5H_4FeC_5H_5$

Complex **2a** has C_s symmetry and in the ^1H NMR spectrum the benzyne protons accordingly show a typical AA'BB' pattern of signals at δ 7.15 (m, 2H) and 6.65 (m, 2H). The ^1H NMR spectrum is independent of temperature but the ^{13}C NMR spectrum reveals that the molecule is in fact fluxional. At room temperature only a broad singlet is seen at δ 200.4 for all the CO groups and on warming this sharpens until at 85 °C a doublet is observed with $^2J(CP) = 12$ Hz, consistent with a rapid scrambling of the CO ligands between the various sites available. On cooling to −80 °C four CO signals evolve at δ 195.9 (s, br), 197.1 (s, br), 199.0 (d, J 29 Hz) and 242.5 (s, br) from the room temperature signal. Reference to Fig. 1 shows that **2a** has six CO environments and it is therefore evident that at −80 °C the molecule is still undergoing some restricted averaging process. It seems likely that, as commonly found in metal carbonyl clusters, this involves rotational exchange within the two $Ru(CO)_3$ groups. Consequently, we attribute the most intense signal at δ 197.1 to the two equivalent $Ru(CO)_3$ groups. It is clear that the low field signal at δ 242.5 is due to the μ-CO group and the remaining signals at δ 199.0 and 195.9 are then attributable to the two pairs of equivalent carbonyls in the $Ru(CO)_2$ groups. One of these pairs is effectively *cis* to the phosphorus and one *trans*, allowing the assignment of the ^{31}P-coupled doublet signal at δ 199.0 to the latter.

As suggested for other square tetranuclear metal carbonyls [21], the rapid migration of all the CO groups about the edges of the Ru_4 cluster at room temperature and above is probably due to a "merry-go-round" mechanism, as outlined in Scheme 1. Scheme 1 also reveals the important consequence of these observations, namely that the benzyne must undergo a contra-rotation about the Ru_4 square in order to retain the valence electron count of the metal atoms. Similar benzyne rotation has been established to occur in a 2,3-dimethylbutadiene derivative of **2a**, the complex $[Ru_4(CO)_9(\eta^4\text{-}C_4H_4Me_2)(\mu_4\text{-}PPh)(\mu_4\text{-}\eta^4\text{-}C_6H_4)]$ (**5**). The ^1H NMR spectrum of this species shows an ABCD pattern for the benzyne protons at

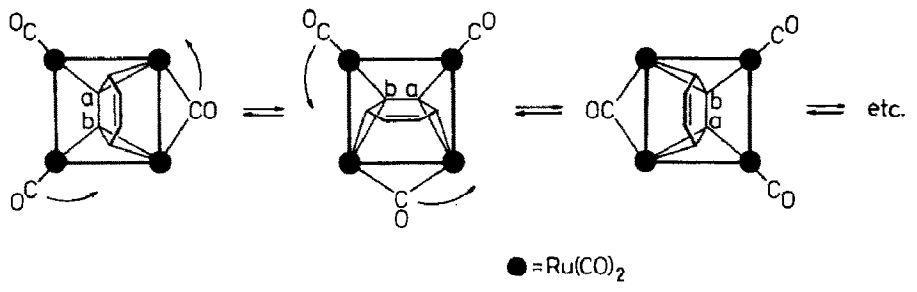

Scheme 1. Proposed CO migration/benzyne rotation process in **2a**.

5 °C, as expected for its asymmetric structure, but at higher temperatures this collapses to an AA′BB′ system, consistent with a benzyne rotation on the Ru_4 centre to generate time-averaged mirror symmetry [22]. The unusually high energy for a CO exchange process in **2a** indicates that the rotation of the benzyne is the rate-limiting factor. Benzyne is thus seen to be capable of rotation on both triangular and square metal centres, in **1** and **2** respectively.

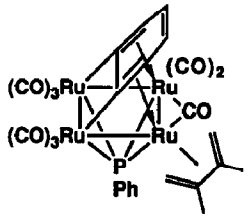

(5)

The ^{13}C NMR signals of the μ_4-η^4-benzyne ligand in **2a** are observed at δ 144.5 (d, J 5 Hz), 128.7 (s), and 121.0 (d, J 5 Hz), assigned to the μ-C, unco-ordinated CH, and co-ordinated CH carbons respectively. The absence of coupling to phosphorus identifies the unco-ordinated CH carbons.

Elemental analyses indicated the pentaruthenium nature of red crystalline $[Ru_5(CO)_{13}(\mu_4\text{-PPh})(\mu_5\text{-}\eta^6\text{-}C_6H_4)]$ (**3a**) while the ^1H NMR spectrum showed, like **2a**, the signals of an AA′BB′ system at δ 5.59 (m, 2H) and 5.83 (m, 2H), consistent with the presence of benzyne. The pattern was, however, shifted to high field compared with that of **2a**, suggesting that the hydrocarbon was now co-ordinated to the additional ruthenium atom. This was supported by the ^{13}C NMR spectrum, which showed the benzyne carbons at δ 153.8 (d, J 8 Hz, μ-C), 89.4 (d, J 3 Hz, CH), and 71.8 (s, CH) respectively; i.e. the carbons of the originally unco-ordinated CH groups of **2a** are now seen more than 50 ppm to higher field. The absence of a μ-CO band in the IR spectrum indicated that the fifth ruthenium might have taken the place of that group in the structure of **2a**. An X-ray diffraction study of **3a** established that this was indeed the case. The molecular structure is shown in Fig. 3 and the results are summarised in Tables 3, 5, 6 and 9.

The view of complex **3a** given in Fig. 3 emphasises the η^2,η^2-η^2-co-ordination of benzyne to the triruthenium unit Ru(3)Ru(4)Ru(5), similar to the bonding of benzene in $[Os_3(CO)_9(C_6H_6)]$ [2]. However, the most striking feature of (**3a**) is that the five ruthenium atoms mimic a step-site on a metal (111) surface (see Scheme 2), where Ru(3)Ru(4)Ru(5) are in one terrace and Ru(1)Ru(2) are step atoms in the first row of the next. Muetterties suggested [1] in 1982 that the dissociative chemisorption (C–H bond cleavage) observed [23] for benzene on a stepped metal (111) surface is due to its η^6-co-ordination parallel to one terrace of the surface allowing a close approach of its hydrogens to the step atoms of a second terrace (see Fig. 8 of ref. 1). Complex **3a** provides attractive support for this idea, in modelling the aftermath of benzene activation on such a surface; i.e. the approach of benzene across a terrace of a (111) surface toward exposed low co-ordinate step atoms is suggested to result in the activation of two *ortho*-C–H bonds, generating benzyne chemisorbed as in **3a**.

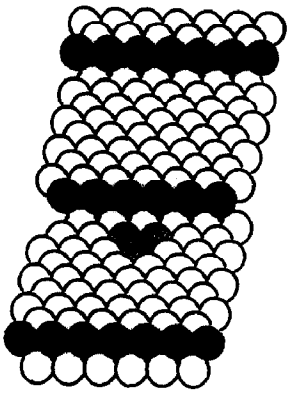

Scheme 2. Representation of a stepped metal (111) surface. The step atoms are shown black. The shaded atoms and adjacent pair of step atoms comprise a five-atom step site of the type found in complex **3a**.

While the concept of benzene C–H activation occurring at a step-site is attractive, it is apparent that C–H activation can also occur at other sites. Recently it was observed that the benzene complex $[Os_3(CO)_9(\eta^6\text{-}C_6H_6)]$ undergoes photochemically induced isomerisation to $[Os_3H_2(CO)_9(\mu_3\text{-}\eta^2\text{-}C_6H_4)]$ [6], containing a μ_3-benzyne ligand of the type found in **1**, indicating that a triangular site is adequate. Whether a square of metal atoms is capable of similar activation is yet to be established, but the co-ordination of benzyne in the complexes **2** could model the dissociative chemisorption of benzene on a metal (100) surface, which is composed of such sites.

Formation of the benzyne complexes

Only two examples exist of a polynuclear benzyne complex being derived from benzene itself: $[Ir_2(CO)_2(\mu\text{-}\eta^2\text{-}C_6H_4)(\eta\text{-}C_5H_5)_2]$ [3] and $[Os_3H_2(CO)_9(\mu_3\text{-}\eta^2\text{-}C_6H_4)]$ [4–6]. Most have been obtained by the thermolysis of a phenylphosphine complex [7–12], and Deeming et al. have shown that the degradation of the phosphine involves *ortho*-metallation followed by phosphorus–carbon bond cleavage [13]. On this basis we suggest (see Scheme 3) that the initial steps in the thermolysis of $[Ru_3(CO)_{11}(PPh_3)]$ are the loss of CO followed by *ortho*-metallation to afford **6**, then the loss of a second CO and co-ordination of a double bond of the C_6H_4 ring to give **7**. The osmium analogue of the latter has been isolated from the thermolysis of $[Os_3(CO)_{11}(PPh_3)]$ [13]. Reaction of **7** with PPh_3 released during the thermolysis would give **8**, and loss of CO from this species, followed by oxidative addition of a P–Ph bond and elimination of benzene, will give **1a**. This sequence is supported by the fact, as mentioned earlier, that **1a** is best obtained by thermolysis of $[Ru_3(CO)_{10}(PPh_3)_2]$, which would be expected to form **8** directly. Heating **1a** alone or with $[Ru_3(CO)_{12}]$ does not give any **2a** or **3a** and a separate pathway is required for the formation of these higher nuclearity species. We suggest that **7** can lose benzene to give **9**, parallelling the behaviour of its osmium analogue [13], and that **2a** and **3a** then arise via step-wise incorporation of ruthenium carbonyl fragments present in solution from the disintegration of $[Ru_3(CO)_{11}(PPh_3)]$. Strong circumstantial evidence for the intermediacy of **9** comes from the thermolysis of $[Ru_3(CO)_{11}(PPh_2Me)]$, described below; this gives a hexaruthenium complex which

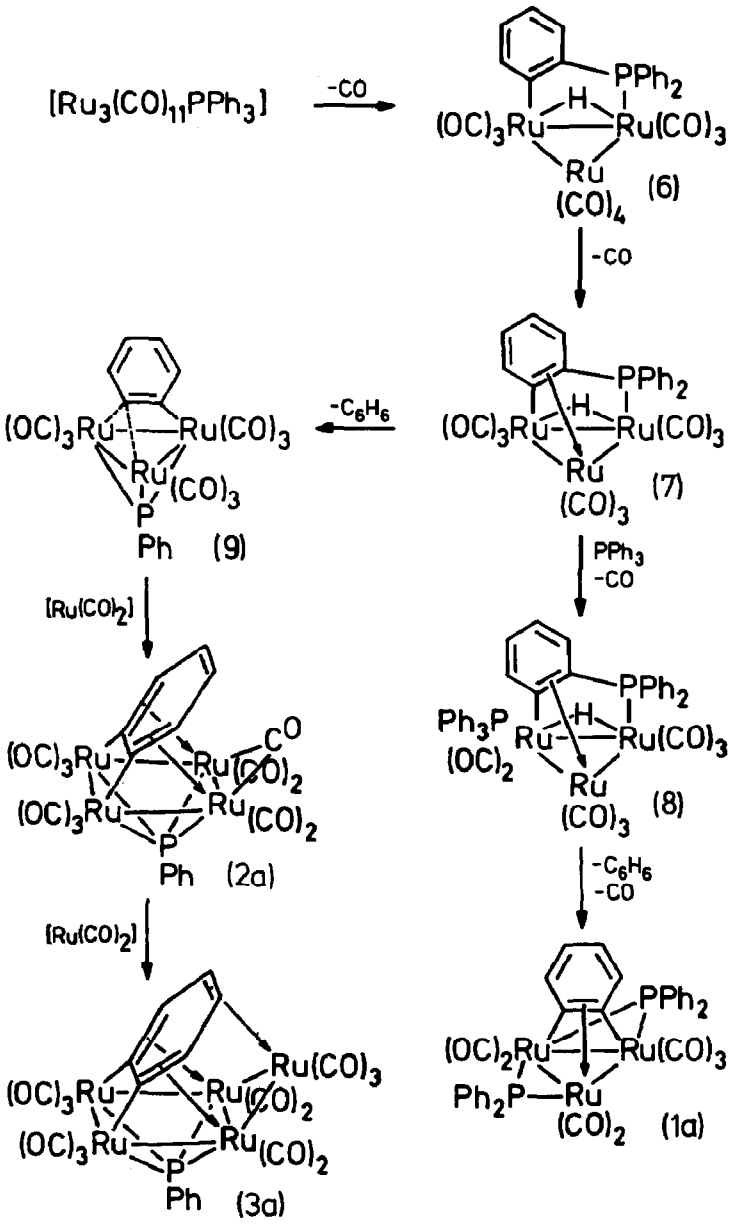

Scheme 3. Proposed formation pathways for benzyne complexes.

can be viewed as arising via "dimerisation" of the μ_3-PMe analogue of **9**. The close structural relationship between the complexes **2a** and **3a** suggests that the latter is formed through the replacement of μ-CO in the former by $Ru(CO)_3$. This is supported by the formation of **3a** in low yield (ca. 2%) when **2a** is heated with $[Ru_3(CO)_{12}]$ in toluene. However, an effort to increase the yield of **3a** by adding $[Ru_3(CO)_{12}]$ to the original reaction mixture had no significant effect.

In an attempt to obtain μ_4-PMe complexes of types **2** and **3** the diphenylmethylphosphine complex $[Ru_3(CO)_{11}(PPh_2Me)]$ was heated in octane for 2.5 h. No evidence for either of these species was found, the main products being $[Ru_3(CO)_{12}]$,

the known $[Ru_5(CO)_{15}(\mu_4\text{-PMe})]$ (**10a**) [24] and a new dark purple hexa-ruthenium complex $[Ru_6(CO)_{12}(\mu\text{-PMe})_2(\mu_3\text{-}\eta^2\text{-}C_6H_4)_2]$ (**11**) in 10% yield. This formulation

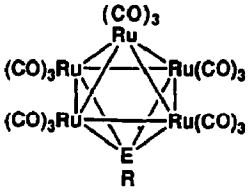

(10a) ER = PMe
(10b) ER = AsPh

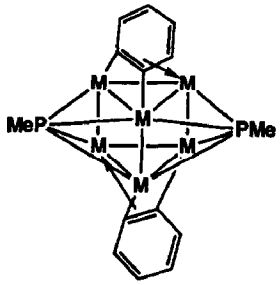

(11) M = $Ru(CO)_2$

was indicated by elemental analyses and the FAB mass spectrum, which showed the molecular ion. The presence of equivalent μ_4-PMe groups was revealed by the ^{31}P NMR spectrum (singlet at δ 520.9) and of equivalent *static* $\mu_3\text{-}\eta^2$-benzyne ligands by the ^1H NMR spectrum [signals at δ 8.32 (d, J 9 Hz, 2H), 8.05 (d, J 9 Hz, 2H), 7.16 (m, 4H) in an ABCD pattern]. These structural features and the evident C_2 molecular symmetry were confirmed by an X-ray diffraction study; the structure is shown in Fig. 4 and the results are summarised in Tables 4, 5, 6 and 10. Discussion of the structure is presented later.

As mentioned earlier, complex **11** can be envisaged to form via the "dimerisation", with associated loss of CO ligands, of the μ_3-PMe analogue of **9** (see Scheme 3). The absence of such a product in the thermolysis of $[Ru_3(CO)_{11}(PPh_3)]$ is attributable to the phenyl groups in **9**, which will sterically hinder such "dimerisation".

Benzynes from tolylphosphines

Methyl-substituted benzyne complexes of types **1**, **2** and **3** could be considered as models for the dissociative chemisorption of toluene on a metal surface. Thermolysis of the tritolylphosphine species $[Ru_3(CO)_9(PR_3)_3]$ (R = *m*- or *p*-C_6H_4Me) has been shown to give the methyl-substituted benzyne complexes $[Ru_3(CO)_7\{\mu\text{-}P(C_6H_4Me)_2\}_2(\mu_3\text{-}\eta^2\text{-}C_6H_3\text{-}4\text{-}Me)]$ (**1b**,**1c**) [7]. In order to obtain corresponding methylbenzyne analogues of **2** and **3** the thermolysis of the mono-tritolylphosphine precursors $[Ru_3(CO)_{11}(PR_3)]$ (R = *m*- or *p*-C_6H_4Me) was examined. On heating these in toluene **1b** and **1c** were formed in about 10% yields, respectively, as expected, but the tetra-ruthenium complex $[Ru_4(CO)_{11}(\mu_4\text{-}PC_6H_4Me)(\mu_4\text{-}\eta^4\text{-}C_6H_3Me)]$ (**2c** or **2d**) was the major product (ca 40%) in each case. No penta-ruthenium benzyne complexes were observed. Interestingly, the ^1H NMR spectra of **1b**, **1c**, **2c** and **2d** show that the same benzyne ligand is present in each complex, i.e. the methyl group is in the 4-position. It is evident that the *ortho*-metallation process involved in the thermolysis of the *para*-substituted phosphine must lead to this configuration, but *ortho*-metallation of the *meta*-substituted phosphine could in principle lead to either the observed 4-substitution or to 3-substitution. Similar observations have been made for the thermolysis of substituted phenylarsine complexes $[Os_3(CO)_{11}(AsMe_2C_6H_4R)]$ (R = Me, OMe); heating $[Os_3(CO)_{11}(AsMe_2C_6H_4\text{-}o\text{-}Me)]$ gave, as here, only the 4-substituted benzyne product, while $[Os_3(CO)_{11}(AsMe_2C_6H_4\text{-}p\text{-}OMe)]$ gave the 3-substituted benzyne [25]. This was attributed to reversible hydrogen transfer between the benzyne and the metal, a

process recently confirmed by Kneuper and Shapley [26]. We conclude that a related situation exists for the ruthenium system.

Benzynes from phenylarsines

It has previously been shown that heating $[Os_3(CO)_{12}]$ with $AsMe_2Ph$ results in the cleavage of the phenyl group from arsenic, to generate the μ_3-benzyne complex $[Os_3(CO)_7(\mu\text{-}AsMe_2)_2(\mu_3\text{-}\eta^2\text{-}C_6H_4)]$ of type **1** [10]. We were surprised, therefore, to observe that the $AsPh_2$ analogue was not* formed on thermolysis of $[Ru_3(CO)_{11}(AsPh_3)]$ in toluene; however, the μ_4- and μ_5-benzyne complexes $[Ru_4(CO)_{10}(\mu\text{-}CO)(\mu_4\text{-}AsPh)(\mu_4\text{-}\eta^4\text{-}C_6H_4)]$ (**2e**) and $[Ru_5(CO)_{13}(\mu_4\text{-}AsPh)(\mu_5\text{-}\eta^6\text{-}C_6H_4)]$ (**3b**) were isolated in 6 and 5% yields, respectively, and readily characterised by comparison of their spectra with those of their phosphorus analogues. The major

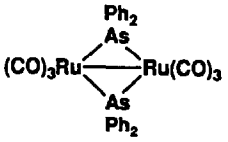

(12)

product (65%) was the yellow crystalline diruthenium complex $[Ru_2(CO)_6(\mu\text{-}AsPh_2)_2]$ (**12**) which may, in view of the absence of $[Ru_3(CO)_7(\mu\text{-}AsPh_2)_2(\mu_3\text{-}\eta^2\text{-}C_6H_4)]$, arise via the decomposition of the latter. A trace of $[Ru_5(CO)_{15}(\mu_4\text{-}AsPh)]$ (**10b**) was identified by IR as a co-product of the thermolysis.

X-ray discussion

Perspective views of the molecular structures of **2a**, **2b**, **3a** and **11** are given in Fig. 1–4, respectively. Tables 1–4 list selected bond lengths and angles for the four structures. Their crystal structures consist of isolated molecules separated by normal van der Waals contacts, there being two crystallographically distinct but structurally similar molecules in each of **2a** and **11**. Each of the molecules **2a** and **2b** consists of an approximately square Ru_4 unit symmetrically bridged on one face of the square by a μ_4-PR group (R = Ph in **2a**, CH_2NPh_2 in **2b**), and by a benzyne ligand on the other. One edge of the Ru_4 unit is bridged by a carbonyl ligand. Two of the four ruthenium atoms carry three terminal carbonyls, those bridged by the μ-CO carry two apiece. The molecular structure of **3a** may be formally derived from that of **2a** by replacement of the μ-CO ligand by an $Ru(CO)_3$ unit which is η^2-bonded to the benzyne ligand. The hexa-metal cluster **11** may be viewed as having a slipped trigonal prismatic Ru_6 core, in which two of the quadrilateral faces of the prism are bridged by the μ_4-PPh groups, while the third has a diagonal Ru–Ru bond [Ru(11)–Ru(14) in the first molecule, and Ru(21)–Ru(24) in the second]. The ruthenium atoms each carry two terminal carbonyl ligands apiece. The triangular faces of the Ru_6 prism are each bridged by a μ_3-benzyne ligand of the same type as in **1a** [8].

In species **2** the benzyne ligand acts as a neutral six-electron donor by σ-bonds to Ru(1) and Ru(2) and π-bonds to Ru(3) and Ru(4). In **3a**, as a result of the extra η^2-interaction with Ru(5), the benzyne is an eight-electron donor. In **11** the benzynes act as four-electron donors. The cluster valence electron counts in **2a**, **2b**, **3a** and **11** are 64, 64, 78, and 88, respectively. The effective atomic number rule therefore

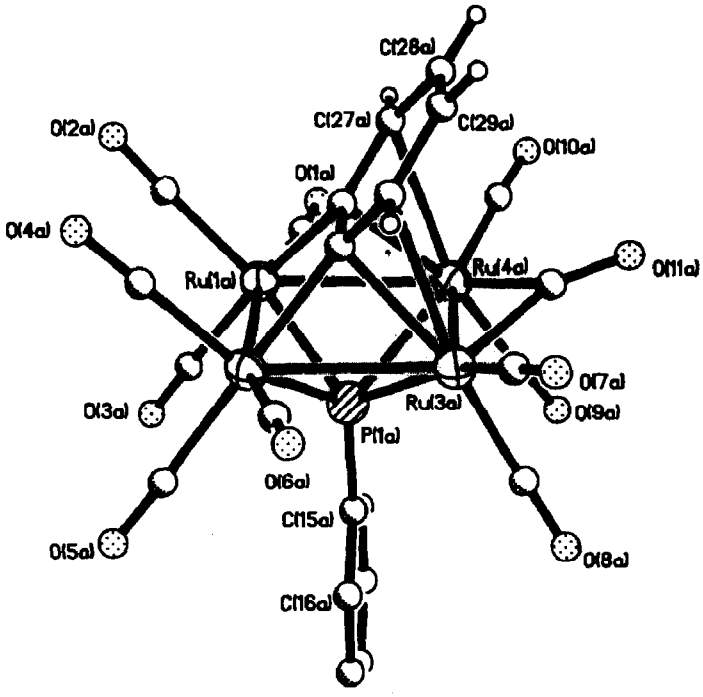

Fig. 1. Molecular structure of one of the two independent molecules of **2a**, showing atom labelling scheme. Phenyl group hydrogens have been omitted for clarity. Metal atoms are represented as ellipsoids enclosing 50% probability density, other atoms as spheres of arbitrary radii.

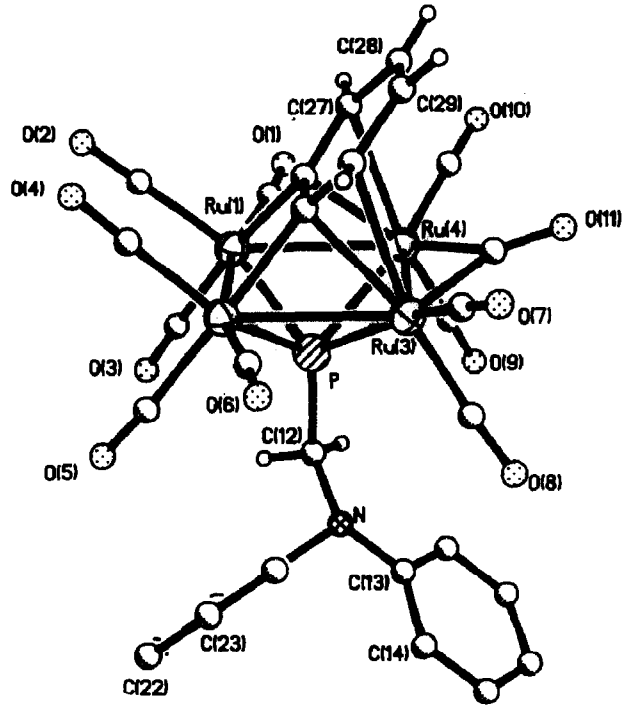

Fig. 2. Molecular structure of **2b**, showing atom labelling scheme. Phenyl group hydrogens have been omitted for clarity. Metal atoms are represented as ellipsoids enclosing 50% probability density, other atoms as spheres of arbitrary radii.

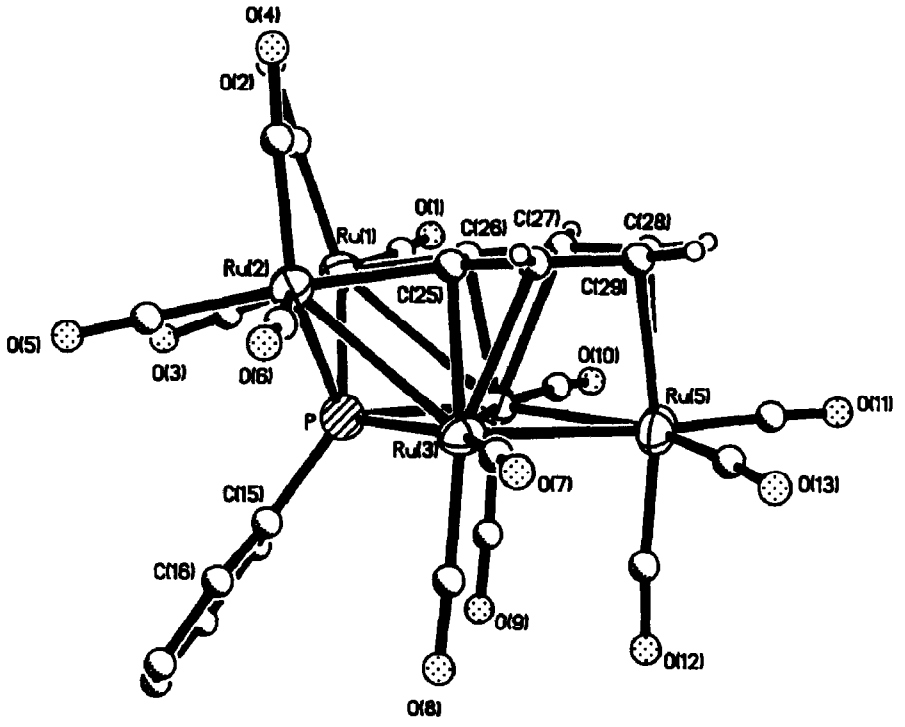

Fig. 3. Molecular structure of **3a**, showing atom labelling scheme. Phenyl group hydrogens have been omitted for clarity. Metal atoms are represented as ellipsoids enclosing 50% probability density, other atoms as spheres of arbitrary radii. Ruthenium atom Ru(4) is partially obscured by Ru(3).

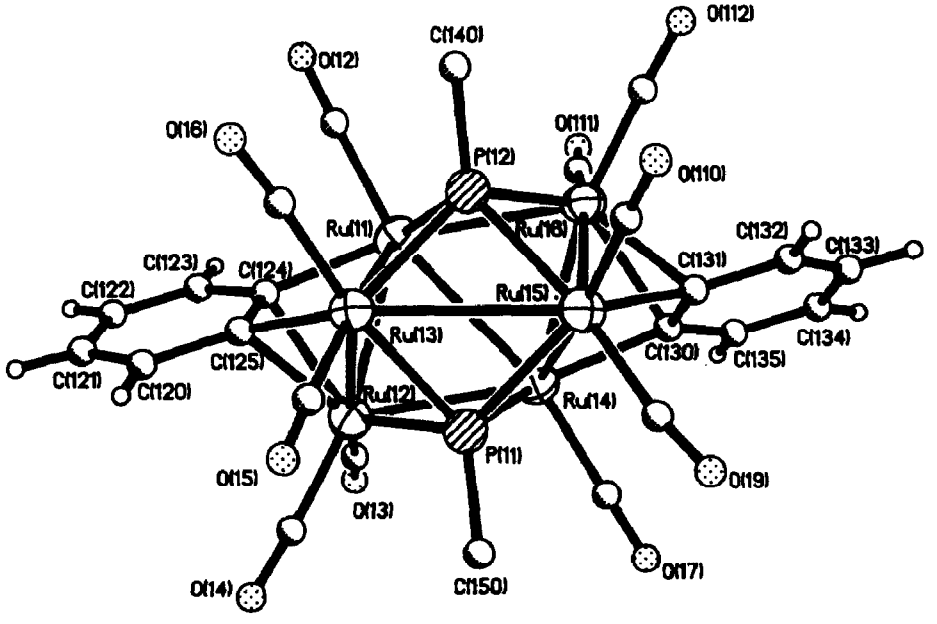

Fig. 4. Molecular structure of one of the two independent molecules of **11**, showing atom labelling scheme. Methyl group hydrogens have been omitted for clarity. Metal atoms are represented as ellipsoids enclosing 50% probability density, other atoms as spheres of arbitrary radii. Two carbonyl ligands, on Ru(11) and Ru(14), are obscured.

Table 1

Bond lengths (Å) and angles (°) for 2a

Ru(1a)–Ru(2a)	2.943(1)	Ru(3b)–C(25b)	2.309(12)	O(9a)–C(9a)	1.135(14)
Ru(1a)–P(1a)	2.352(3)	Ru(4b)–P(1b)	2.432(3)	O(11a)–C(11a)	1.168(13)
Ru(1a)–C(2a)	1.941(10)	Ru(4b)–C(10b)	1.897(16)	C(15a)–C(20a)	1.354(17)
Ru(1a)–C(26a)	2.108(10)	Ru(4b)–C(26b)	2.317(13)	C(17a)–C(18a)	1.355(20)
Ru(2a)–P(1a)	2.353(3)	P(1b)–C(15b)	1.812(11)	C(19a)–C(20a)	1.380(16)
Ru(2a)–C(5a)	1.969(11)	O(2b)–C(2b)	1.137(19)	C(25a)–C(30a)	1.403(16)
Ru(2a)–C(25a)	2.110(10)	O(4b)–C(4b)	1.138(18)	C(27a)–C(28a)	1.399(18)
Ru(3a)–P(1a)	2.425(3)	O(6b)–C(6b)	1.139(13)	C(29a)–C(30a)	1.405(16)
Ru(3a)–C(8a)	1.886(10)	O(8b)–C(8b)	1.119(16)	Ru(1b)–Ru(4b)	2.910(2)
Ru(3a)–25a)	2.294(9)	O(10b)–C(10)	1.131(20)	Ru(1b)–C(1b)	1.870(16)
Ru(4a)–P(1a)	2.446(3)	C(15b)–C(16b)	1.388(15)	Ru(1b)–C(3b)	1.946(12)
Ru(4a)–C(10a)	1.896(11)	C(16b)–C(17b)	1.380(18)	Ru(2b)–Ru(3b)	2.918(1)
Ru(4a)–C(26a)	2.299(10)	C(18b)–C(19b)	1.371(20)	Ru(2b)–C(4b)	1.924(14)
P(1a)–C(15a)	1.823(10)	C(25b)–C(26b)	1.460(16)	Ru(2b)–C(6b)	1.898(11)
O(2a)–C(2a)	1.112(13)	C(26b)–C(27b)	1.419(18)	Ru(3b)–Ru(4b)	2.805(1)
O(4a)–C(4a)	1.123(13)	C(28b)–C(29b)	1.355(25)	Ru(3b)–C(7b)	1.907(13)
O(6a)–C(6a)	1.124(15)	Ru(1a)–Ru(4a)	2.891(1)	Ru(3b)–C(11b)	2.076(13)
O(8a)–C(8a)	1.113(13)	Ru(1a)–C(1a)	1.889(12)	ru(3b)–C(30b)	2.583(12)
O(10a)–C(10a)	1.145(14)	Ru(1a)–C(3a)	1.947(11)	Ru(4b)–C(9b)	1.847(14)
C(15a)–C(16a)	1.387(14)	Ru(2a)–Ru(3a)	2.896(1)	Ru(4b)–C(11b)	2.065(12)
C(16a)–C(17a)	1.391(17)	Ru(2a)–C(4a)	1.910(11)	Ru(4b)–C(27b)	2.619(14)
C(18a)–C(19a)	1.374(18)	Ru(2a)–C(6a)	1.913(12)	O(1b)–C(1b)	1.153(20)
C(25a)–C(26a)	1.455(15)	Ru(3a)–Ru(4a)	2.791(11)	O(3b)–C(3b)	1.125(15)
C(26a)–C(27a)	1.395(14)	Ru(3a)–C(7a)	1.903(13)	O(5b)–C(5b)	1.135(15)
C(28a)–C(29a)	1.360(20)	Ru(3a)–C(11a)	2.066(11)	O(7b)–C(7b)	1.131(16)
Ru(1b)–Ru(2b)	2.932(1)	Ru(3a)–C(30a)	2.656(11)	O(9b)–C(9b)	1.153(18)
Ru(1b)–P(1b)	2.344(3)	Ru(4a)–C(9a)	1.866(11)	O(11b)–C(11b)	1.167(15)
Ru(1b)–C(2b)	1.928(15)	Ru(4a)–C(11a)	2.050(12)	C(15b)–C(20b)	1.382(16)
Ru(1b)–C(26b)	2.100(11)	Ru(4a)–C(27a)	2.689(11)	C(17b)–C(18b)	1.385(20)
Ru(2b)–P(1b)	2.354(4)	O(1a)–C(1a)	1.145(15)	C(19b)–C(20b)	1.359(18)
Ru(2b)–C(5b)	1.945(12)	O(3a)–C(3a)	1.109(14)	C(25b)–C(30b)	1.393(14)
Ru(2b)–C(25b)	2.122(10)	O(5a)–C(5a)	1.111(140	C(27b)–C(28b)	1.394(20)
Ru(3b)–P(1b)	2.444(3)	O(7a)–C(7a)	1.130(17)	C(29b)–C(30b)	1.373(20)
Ru(3b)–C(8b)	1.889(13)				

Ru(1a)–P(1a)–Ru(2a)	77.5(1)	Ru(1a)–P(1a)–Ru(3a)	116.7(1)
Ru(2a)–P(1a)–Ru(3a)	74.6(1)	Ru(1a)–P(1a)–Ru(4a)	74.1(1)
Ru(2a)–P(1a)–Ru(4a)	116.4(1)	Ru(3a)–P(1a)–Ru(4a)	69.9(1)
Ru(1a)–P(1a)–C(15a)	121.5(3)	Ru(2a)–P(1a)–C(15a)	125.3(3)
Ru(3a)–P(1a)–C(15a)	121.2(3)	Ru(4a)–P(1a)–C(15a)	118.1(3)
Ru(1a)–C(1a)–O(1a)	172.9(10)	Ru(1a)–C(2a)–O(2a)	117.0(10)
Ru(1a)–C(3a)–O(3a)	178.7(10)	Ru(2a)–C(4a)–O(4a)	179.2(12)
Ru(2a)–C(5a)–O(5a)	176.5(11)	Ru(2a)–C(6a)–O(6a)	176.2(9)
Ru(3a)–C(7a)–O(7a)	177.6(10)	Ru(3a)–C(8a)–O(8a)	177.5(12)
Ru(4a)–C(9a)–O(9a)	177.0(10)	Ru(4a)–C(10a)–O(10a)	176.7(10)
Ru(3a)–C(11a)–Ru(4a)	85.4(4)	Ru(3a)–C(11a)–O(11a)	135.5(10)
Ru(4a)–C(11a)–O(11a)	139.2(9)	P(1a)–C(15a)–C(16a)	120.3(9)
P(1a)–C(15a)–C(20a)	119.5(7)	C(16a)–C(15a)–C(20a)	120.2(10)
C(15a)–C(16a)–C(17a)	118.0(12)	C(16a)–C(17a)–C(18a)	121.7(11)
C(17a)–C(18a)–C(19a)	119.6(12)	C(18a)–C(19a)–C(20a)	119.5(13)
C(15a)–C(20a)–C(19a)	121.0(11)	Ru(2a)–C(25a)–Ru(3a)	82.1(3)
Ru(2a)–C(25a)–C(26a)	111.3(7)	Ru(3a)–C(25a)–C(26a)	107.9(7)
Ru(2a)–C(25a)–C(30a)	130.2(8)	Ru(3a)–C(25a)–C(30a)	88.4(6)
C(26a)–C(25a)–C(30a)	118.1(9)	Ru(1a)–C(26a)–Ru(4a)	81.9(4)
Ru(1a)–C(26a)–C(25a)	110.0(7)	Ru(4a)–C(26a)–C(25a)	105.9(6)

Table 1 (continued)

Ru(1a)–C(26a)–C(27a)	132.2(8)	Ru(4a)–C(26a)–C(27a)	90.0(7)
C(25a)–C(26a)–C(27a)	117.5(10)	Ru(4a)–C(27a)–C(26a)	58.8(6)
Ru(4a)–C(27a)–C(28a)	118.5(7)	C(26a)–C(27a)–C(28a)	123.0(11)
C(27a)–C(28a)–C(29a)	119.1(11)	C(28a)–C(29a)–C(30a)	120.8(12)
Ru(3a)–C(30a)–C(25a)	59.7(5)	Ru(3a)–C(30a)–C(29a)	120.1(8)
C(25a)–C(30a)–C(29a)	121.4(12)	Ru(1b)–P(1b)–Ru(2b)	77.2(1)
Ru(1b)–P(1b)–Ru(3b)	117.4(1)	Ru(2b)–P(1b)–Ru(3b)	74.9(1)
Ru(1b)–P(1b)–Ru(4b)	75.1(1)	Ru(2b)–P(1b)–Ru(4b)	117.2(1)
Ru(3b)–P(1b)–Ru(4b)	70.2(1)	Ru(1b)–P(1b)–C(15b)	123.5(4)
Ru(2b)–P(1b)–C(15b)	124.5(4)	Ru(3b)–P(1b)–C(15b)	118.6(4)
Ru(4b)–P(1b)–C(15b)	117.9(4)	Ru(1b)–C(1b)–O(1b)	174.9(17)
Ru(1b)–C(2b)–O(2b)	178.8(12)	Ru(1b)–C(3b)–O(3b)	177.3(12)
Ru(2b)–C(4b)–O(4b)	178.0(11)	Ru(2b)–C(5b)–O(5b)	178.6(12)
Ru(2b)–C(6b)–O(6b)	174.8(11)	Ru(3b)–C(7b)–O(7b)	175.3(13)
Ru(3b)–C(8b)–O(8b)	175.3(11)	Ru(4b)–C(9b)–O(9b)	178.0(11)
Ru(4b)–C(10b)–O(10b)	175.3(15)	Ru(3b)–C(11b)–Ru(4b)	85.3(5)
Ru(3b)–C(11b)–O(11b)	135.1(10)	Ru(4b)–C(11b)–O(11b)	139.6(10)
P(1b)–C(15b)–C(16b)	121.0(8)	P(1b)–C(15b)–C(20b)	121.9(8)
C(16b)–C(15b)–C(20b)	117.0(10)	C(15b)–C(16b)–C(17b)	121.1(11)
C(16b)–C(17b)–C(18b)	119.6(12)	C(17b)–C(18b)–C(19b)	119.9(12)
C(18b)–C(19b)–C(20b)	119.4(12)	C(15b)–C(20b)–C(19b)	122.8(11)
Ru(2b)–C(25b)–Ru(3b)	82.2(4)	Ru(2b)–C(25b)–C(26b)	109.3(7)
Ru(3b)–C(25b)–C(26b)	107.6(8)	Ru(2b)–C(25b)–C(30b)	131.8(9)
Ru(3b)–C(25b)–C(30b)	84.6(7)	C(26b)–C(25b)–C(30b)	118.9(10)
Ru(1b)–C(26b)–Ru(4b)	82.3(4)	Ru(1b)–C(26b)–C(25b)	111.5(8)
Ru(4b)–C(26b)–C(25b)	106.2(8)	Ru(1b)–C(26b)–C(27b)	131.3(9)
Ru(4b)–C(26b)–C(27b)	85.4(9)	C(25b)–C(26b)–C(27b)	117.1(10)
Ru(4b)–C(27b)–C(25b)	61.9(7)	Ru(4b)–C(27b)–C(28b)	114.0(11)
C(26b)–C(27b)–C(28b)	120.5(13)	C(27b)–C(28b)–C(29b)	121.2(14)
C(28b)–C(29b)–C(30b)	120.8(13)	Ru(3b)–C(30b)–C(25b)	62.9(6)
Ru(3b)–C(30b)–C(29b)	115.4(10)	C(25b)–C(30b)–C(29b)	121.4(12)

predicts numbers of metal–metal bonds 4, 4, 6, and 10 respectively, as observed. The lengths of the metal–metal bonds are highly variable, ranging from 2.720(1) to 3.166(1) Å. There is notable variation between the chemically identical but crystallographically distinct molecules in each of **2a** and **11** (rms difference in equivalent Ru–Ru bond lengths being 0.017 Å for **2a** and 0.024 Å for **11**). The shorter Ru–Ru distances (< 2.8 Å) are, for the most part, between ruthenium atoms bridged by carbon atoms, of carbonyl ligands in **2a** and **2c** or of a benzyne ligand. The longer Ru–Ru distances are, for the most part, bridged by the μ_4-PR ligands, most notably Ru(13)–Ru(15) and Ru(23)–Ru(25) in **4**, which are the longest Ru–Ru bond lengths, at 3.143(1) and 3.166(1) Å, respectively, and are doubly bridged by phosphinidene ligands.

Details of the co-ordination of the μ_n-benzyne (n = 3, 4, or 5) ligands in **1a** [8], **2a**, **2b**, **3a** and **11** are given in Table 5. In each case the benzyne is co-ordinated to two metal atoms by σ-bonds lying close to the plane of the C_6 ring. This plane is inclined at an acute angle to the Ru_3 or Ru_4 plane. As indicated in Table 5 there is considerable flexibility in this angle, which varies from 41.8 to 73.4°, reflecting the softness of the π-interactions in **2a** and **2b**. The logical extension of this flexibility, leading to an interplanar angle of near 90°, has been observed in the μ_4-benzyne

Table 2

Bond lengths (Å) and angles (°) for **2b**

Ru(1)–Ru(2)	2.921(1)	C(16)–H(5)	0.957(57)	Ru(4)–C(27)	2.592(4)
Ru(1)–P	2.359(1)	C(17)–H(6)	0.895(35)	N–C(12)	1.458(5)
Ru(1)–C(2)	1.928(5)	C(19)–C(20)	1.384(6)	N–C(19)	1.438(5)
Ru(1)–C(26)	2.115(4)	C(20–C(21)	1.375(7)	O(2)–C(2)	1.130(7)
Ru(2)–P	2.356(1)	C(21)–C(22)	1.370(10)	O(4)–C(4)	1.131(7)
Ru(2)–C(5)	1.951(4)	C(22)–C(23)	1.362(10)	O(6)–C(6)	1.134(6)
Ru(2)–C(25)	2.117(3)	C(23)–C(24)	1.382(8)	O(8)–C(8)	1.139(5)
Ru(3)–P	2.423(1)	C(24)–H(12)	0.890(40)	O(10)–C(10)	1.127(5)
Ru(3)–C(8)	1.871(4)	C(25)–C(30)	1.402(5)	C(12)–H(1)	0.873(35)
Ru(3)–C(25)	2.301(4)	C(27)–C(28)	1.427(6)	C(13)–C(14)	1.403(5)
Ru(4)–P	2.469(1)	C(28)–C(29)	1.344(6)	C(14)–C(15)	1.371(7)
Ru(4)–C(10)	1.902(4)	C(29)–C(30)	1.407(6)	C(15)–C(16)	1.380(7)
Ru(4)–C(26)	2.292(4)	C(30)–H(16)	0.902(35)	C(16)–C(17)	1.367(7)
P–C(12)	1.871(4)	Ru(1)–Ru(4)	2.875(1)	C(17)–C(18)	1.388(7)
N–C(13)	1.407(5)	Ru(1)–C(1)	1.911(4)	C(18)–H(7)	0.941(39)
O(1)–C(1)	1.129(5)	Ru(1)–C(3)	1.945(4)	C(19)–C(24)	1.365(6)
O(3)–C(3)	1.121(6)	Ru(2)–Ru(3)	2.927(1)	C(20)–H(8)	0.851(44)
O(5)–C(5)	1.124(5)	Ru(2)–C(4)	1.926(5)	C(21)–H(9)	1.028(61)
O(7)–C(7)	1.134(6)	Ru(2)–C(6)	1.902(4)	C(22)–H(10)	0.884(69)
O(9)–C(9)	1.139(5)	Ru(3)–Ru(4)	2.816(1)	C(23)–H(11)	0.759(57)
O(11)–C(11)	1.167(5)	Ru(3)–C(7)	1.904(4)	C(25)–C(26)	1.447(5)
C(12)–H(2)	0.907(42)	Ru(3)–C(11)	2.075(4)	C(26)–C(27)	1.391(5)
C(13)–C(18)	1.392(5)	Ru(3)–C(30)	2.634(4)	C(27)–H(13)	0.880(29)
C(14)–H(3)	0.835(41)	Ru(4)–C(9)	1.863(4)	C(28)–(14)	0.922(44)
C(15)–H(4)	0.888(42)	Ru(4)–C(11)	2.066(4)	C(29)–H(15)	0.936(45)

Ru(1)–P–Ru(2)	76.6(1)	Ru(1)–P–Ru(3)	117.0(1)
Ru(2)–P–Ru(3)	75.5(1)	Ru(1)–P–Ru(4)	73.1(1)
Ru(2)–P–Ru(4)	115.5(1)	Ru(3)–P–Ru(4)	70.3(1)
Ru(1)–P–C(12)	119.1(1)	Ru(2)–P–C(12)	124.6(1)
Ru(3)–P–C(12)	123.3(1)	Ru(4)–P–C(12)	119.9(1)
C(12)–N–C(13)	121.4(3)	C(12)–N–C(19)	114.1(3)
C(13)–N–C(19)	117.0(3)	Ru(1)–C(1)–O(1)	173.9(5)
Ru(1)–C(2)–O(2)	179.1(4)	Ru(1)–C(3)–O(3)	178.9(4)
Ru(2)–C(4)–O(4)	178.9(4)	Ru(2)–C(5)–O(5)	173.7(4)
Ru(2)–C(6)–O(6)	174.7(4)	Ru(3)–C(7)–O(7)	177.5(5)
Ru(3)–C(8)–O(8)	175.1(4)	Ru(4)–C(9)–O(9)	177.0(4)
Ru(4)–C(10)–O(10)	178.2(4)	Ru(3)–C(11)–Ru(4)	85.7(2)
Ru(3)–C(11)–O(11)	136.7(3)	Ru(4)–C(11)–O(11)	137.6(3)
P–C(12)–N	116.5(3)	P–C(12)–H(1)	104.6(23)
N–C(12)–H(1)	112.6(24)	P–C(12)–H(2)	104.8(26)
N–C(12)–H(2)	112.6(22)	H(1)–C(12)–H(2)	104.6(35)
		Ru(2)–C(25)–Ru(3)	82.9(1)
Ru(2)–C(25)–C(26)	108.7(2)	Ru(3)–C(25)–C(26)	108.0(2)
Ru(2)–C(25)–C(30)	132.2(3)	Ru(3)–C(25)–C(30)	87.1(2)
C(26)–C(25)–C(30)	118.8(3)	Ru(1)–C(26)–Ru(4)	81.3(1)
Ru(1)–C(26)–C(25)	112.0(2)	Ru(4)–C(26)–C(25)	106.7(3)
Ru(1)–C(26)–C(27)	130.3(3)	Ru(4)–C(26)–C(27)	85.8(2)
C(25)–C(26)–C(27)	117.7(3)	Ru(4)–C(27)–C(26)	61.9(2)
Ru(4)–C(27)–C(28)	115.7(3)	C(26)–C(27)–C(28)	121.8(3)
Ru(4)–C(27)–H(13)	99.5(22)	C(26)–C(27)–H(13)	122.1(22)
C(28)–C(27)–H(13)	115.7(22)	C(27)–C(28)–C(29)	119.8(4)
C(27)–C(28)–H(14)	117.9(29)	C(29)–C(28)–H(14)	122.2(29)
C(28)–C(29)–C(30)	120.6(4)	C(28)–C(29)–H(15)	118.0(23)
C(30)–C(29)–H(15)	121.4(24)	Ru(3)–C(30)–C(25)	60.7(2)
Ru(3)–C(30)–C(29)	116.9(3)	C(25)–C(30)–C(29)	121.1(3)

Table 3

Bond lengths (Å) and angles (°) for **3a**

Ru(1)–Ru(2)	2.902(1)	O(11)–C(11)	1.126(12)	Ru(4)–P	2.381(2)
Ru(1)–P	2.379(1)	O(13)–C(13)	1.137(10)	Ru(4)–C(10)	1.889(7)
Ru(1)–C(2)	1.906(7)	C(15)–C(20)	1.382(9)	Ru(4)–C(27)	2.390(6)
Ru(1)–C(26)	2.097(6)	C(17)–C(18)	1.378(11)	Ru(5)–C(12)	1.865(7)
Ru(2)–P	2.386(2)	C(19)–C(20)	1.372(9)	Ru(5)–C(28)	2.427(6)
Ru(2)–C(5)	1.951(8)	C(25)–C(30)	1.380(9)	P–C(15)	1.815(6)
Ru(2)–C(25)	2.116(6)	C(27)–H(27)	0.974(58)	O(2)–C(2)	1.137(9)
Ru(3)–Ru(5)	2.769(1)	C(28)–H(28)	0.902(68)	O(4)–C(4)	1.143(9)
Ru(3)–C(7)	1.907(8)	C(29)–H(29)	0.954(73)	O(6)–C(6)	1.125(10)
Ru(3)–C(25)	2.234(5)	C(30)–H(30)	1.019(65)	O(8)–C(8)	1.140(8)
Ru(4)–Ru(5)	2.783(1)	Ru(1)–Ru(4)	2.897(1)	O(10)–C(10)	1.135(9)
Ru(4)–C(9)	1.885(6)	Ru(1)–C(1)	1.900(8)	O(12)–C(12)	1.151(9)
Ru(4)–C(26)	2.251(6)	Ru(1)–C(3)	1.939(7)	C(15)–C(16)	1.387(8)
Ru(5)–C(11)	1.900(9)	Ru(2)–Ru(3)	2.905(1)	C(16)–C(17)	1.394(9)
Ru(5)–C(13)	1.892(8)	Ru(2)–C(4)	1.907(7)	C(18)–C(19)	1.372(10)
Ru(5)–C(29)	2.398(7)	Ru(2)–C(6)	1.905(8)	C(25)–C(26)	1.451(9)
O(1)–C(1)	1.133(10)	Ru(3)–Ru(4)	2.865(1)	C(26)–C(27)	1.395(9)
O(3)–C(3)	1.140(9)	Ru(3)–P	2.378(2)	C(27)–C(28)	1.441(10)
O(5)–C(5)	1.135(10)	Ru(3)–C(8)	1.872(6)	C(28)–C(29)	1.394(10)
O(7)–C(7)	1.130(10)	Ru(3)–C(30)	2.391(5)	C(29)–C(30)	1.443(10)
O(9)–C(9)	1.132(8)				

		Ru(1)–P–Ru(2)	75.0(1)
Ru(1)–P–Ru(3)	118.6(1)	Ru(2)–P–Ru(3)	75.1(1)
Ru(1)–P–Ru(4)	75.0(1)	Ru(2)–P–Ru(4)	118.1(1)
Ru(3)–P–Ru(4)	74.0(1)	Ru(1)–P–C(15)	123.1(2)
Ru(2)–P–C(15)	122.6(2)	Ru(3)–P–C(15)	118.2(2)
Ru(4)–P–C(15)	119.2(2)	Ru(1)–C(1)–O(1)	175.2(7)
Ru(1)–C(2)–O(2)	177.3(8)	Ru(1)–C(3)–O(3)	179.0(7)
Ru(2)–C(4)–O(4)	176.3(9)	Ru(2)–C(5)–O(5)	174.3(7)
Ru(2)–C(6)–O(6)	174.3(8)	Ru(3)–C(7)–O(7)	178.2(6)
Ru(3)–C(8)–O(8)	178.4(7)	Ru(4)–C(9)–O(9)	177.0(6)
Ru(4)–C(10)–O(10)	176.6(6)	Ru(5)–C(11)–O(11)	177.5(7)
Ru(5)–C(12)–O(21)	173.8(7)	Ru(5)–C(13)–O(13)	176.2(7)
P–C(15)–C(16)	119.9(5)	P–C(15)–C(20)	120.9(4)
C(16)–C(15)–C(20)	119.2(5)	C(15)–C(16)–C(17)	119.9(6)
C(16)–C(17)–C(18)	119.8(6)	C(17)–C(18)–C(19)	120.2(6)
C(18)–C(19)–C(20)	120.2(7)	C(15)–C(20)–C(19)	120.7(6)
Ru(2)–C(25)–Ru(3)	83.8(2)	Ru(2)–C(25)–C(26)	108.1(4)
Ru(3)–C(25)–C(26)	108.8(4)	Ru(2)–C(25)–C(30)	130.7(5)
Ru(3)–C(25)–C(30)	79.0(3)	C(26)–C(25)–C(30)	121.2(6)
Ru(1)–C(26)–Ru(4)	83.5(2)	Ru(1)–C(26)–C(25)	112.2(4)
Ru(4)–C(26)–C(25)	107.9(3)	Ru(1)–C(26)–C(27)	129.2(5)
Ru(4)–C(26)–C(27)	78.0(4)	C(25)–C(26)–C(27)	118.4(6)
Ru(4)–C(27)–C(26)	67.1(3)	Ru(4)–C(27)–H(27)	98.8(34)
C(26)–C(27)–H(27)	120.6(38)	Ru(4)–C(27)–C(28)	109.5(4)
C(26)–C(27)–C(28)	120.7(6)	H(27)–C(27)–C(28)	118.3(38)
Ru(5)–C(28)–C(27)	102.9(4)	Ru(5)–C(28)–H(28)	100.1(39)
C(27)–C(28)–H(28)	121.7(42)	Ru(5)–C(28)–C(29)	72.1(4)
C(27)–C(28)–C(29)	119.8(6)	H(28)–C(28)–C(29)	118.1(43)
Ru(5)–C(29)–C(28)	74.3(4)	Ru(5)–C(29)–H(29)	103.9(40)
C(28)–C(29)–H(29)	125.1(39)	Ru(5)–C(29)–C(30)	101.9(4)
C(28)–C(29)–C(30)	119.9(6)	H(29)–C(29)–C(30)	114.2(41)
Ru(3)–C(30)–C(25)	66.5(3)	Ru(3)–C(30)–C(29)	110.3(4)
C(25)–C(30)–C(29)	119.7(6)	Ru(3)–C(30)–H(30)	98.1(31)
C(25)–C(30)–H(30)	118.4(36)	C(29)–C(30)–H(30)	121.5(36)

Table 4

Bond lengths (Å) and angles (°) for **11**

Ru(11)–Ru(12)	2.740(1)	Ru(24)–P(21)	2.337(1)	P(12)–C(140)	1.840(6)
Ru(11)–Ru(14)	2.991(1)	Ru(24)–C(28)	1.895(6)	O(12)–C(12)	1.128(7)
Ru(11)–P(12)	2.323(1)	Ru(25)–Ru(26)	2.739(1)	O(14)–C(14)	1.134(9)
Ru(11)–C(12)	1.911(6)	Ru(25)–P(22)	2.366(1)	O(16)–C(16)	1.143(7)
Ru(12)–Ru(13)	2.739(1)	Ru(25)–C(210)	1.877(6)	O(18)–C(18)	1.145(8)
Ru(12)–P(11)	2.321(1)	Ru(26)–P(22)	2.331(1)	O(110)–C(110)	1.136(8)
Ru(12)–C(14)	1.875(7)	Ru(26)–C(212)	1.878(6)	O(112)–C(12)	1.120(9)
Ru(12)–C(125)	2.215(5)	Ru(26)–C(231)	2.241(5)	C(120)–C(125)	1.436(9)
Ru(13)–P(11)	2.376(1)	P(22)–C(240)	1.836(5)	C(122)–C(123)	1.339(12)
Ru(13)–C(15)	1.881(6)	O(22)–C(22)	1.116(7)	C(124)–C(125)	1.409(8)
Ru(13)–C(125)	2.091(6)	O(24)–C(24)	1.125(7)	C(130)–C(135)	1.431(8)
Ru(14)–Ru(16)	2.731(1)	O(26)–C(26)	1.137(7)	C(135)–C(134)	1.329(10)
Ru(14)–C(17)	1.910(6)	O(28)–C(28)	1.146(8)	C(134)–C(133)	1.410(11)
Ru(14)–C(130)	2.096(6)	O(210)–C(210)	1.134(8)	Ru(21)–Ru(23)	2.897(1)
Ru(15)–P(11)	2.399(2)	O(212)–C(212)	1.120(8)	Ru(21)–Ru(26)	2.859(1)
Ru(15)–C(19)	1.928(6)	C(220)–C(225)	1.444(9)	Ru(21)–C(21)	1.910(6)
Ru(15)–C(131)	2.097(6)	C(222)–C(223)	1.364(10)	Ru(21)–C(224)	2.099(6)
Ru(16)–C(12)	1.874(7)	C(224)–C(225)	1.406(7)	Ru(22)–Ru(24)	2.769(1)
Ru(16)–C(130)	2.198(5)	C(230)–C(235)	1.439(8)	Ru(22)–C(23)	1.889(6)
P(11)–C(150)	1.818(5)	C(232)–C(233)	1.360(10)	Ru(22)–C(224)	2.188(5)
O(11)–C(11)	1.144(8)	C(234)–C(235)	1.334(10)	Ru(23)–P(21)	2.370(1)
O(13)–C(13)	1.139(7)	Ru(11)–Ru(13)	2.915(1)	Ru(23)–C(25)	1.892(6)
O(15)–C(15)	1.164(8)	Ru(11)–Ru(16)	2.819(1)	Ru(23)–C(225)	2.087(6)
O(17)–C(17)	1.124(7)	Ru(11)–C(11)	1.884(6)	Ru(24)–Ru(26)	2.720(1)
O(19)–C(19)	1.110(7)	Ru(11)–C(124)	2.105(6)	Ru(24)–C(27)	1.889(6)
O(111)–C(111)	1.175(8)	Ru(12)–Ru(14)	2.822(1)	Ru(24)–C(230)	2.102(6)
C(120)–C(121)	1.363(10)	Ru(12)–C(13)	1.897(6)	Ru(25)–P(21)	2.400(1)
C(121)–C(122)	1.395(11)	Ru(12)–C(124)	2.216(5)	Ru(25)–C(29)	1.912(5)
C(123)–C(124)	1.427(9)	Ru(13)–Ru(15)	3.143(1)	Ru(25)–C(231)	2.095(6)
C(130)–C(131)	1.404(8)	Ru(13)–P(12)	2.389(2)	Ru(26)–C(211)	1.897(6)
C(131)–C(132)	1.426(10)	Ru(13)–C(16)	1.906(5)	Ru(26)–C(230)	2.195(5)
C(132)–C(133)	1.350(9)	Ru(14)–Ru(15)	2.916(1)	P(21)–C(250)	1.823(5)
Ru(21)–Ru(22)	2.740(1)	Ru(14)–P(11)	2.325(1)	O(21)–C(21)	1.134(8)
Ru(21)–Ru(24)	3.001(1)	Ru(14)–C(18)	1.901(6)	O(23)–C(23)	1.141(7)
Ru(21)–P(22)	2.315(1)	Ru(15)–Ru(16)	2.748(1)	O(25)–C(25)	1.133(8)
Ru(21)–C(22)	1.920(6)	Ru(15)–P(12)	2.365(1)	O(27)–C(27)	1.133(8)
Ru(22)–Ru(23)	2.740(1)	Ru(15)–C(110)	1.881(6)	O(29)–C(29)	1.143(7)
Ru(22)–P(21)	2.319(1)	Ru(16)–P(12)	2.332(1)	O(211)–C(211)	1.123(9)
Ru(22)–C(24)	1.884(6)	Ru(16)–C(111)	1.861(6)	C(220)–C(221)	1.355(9)
Ru(22)–C(225)	2.217(5)	Ru(16)–C(131)	2.208(5)	C(221)–C(222)	1.382(9)
Ru(23)–P(22)	2.400(1)			C(223)–C(224)	1.450(8)
Ru(23)–C(26)	1.911(5)			C(230)–C(231)	1.404(7)
Ru(24)–Ru(25)	2.910(1)			C(231)–C(232)	1.399(9)
				C(233)–C(234)	1.418(10)

Ru(12)–P(11)–Ru(13)	71.3(1)	Ru(12)–P(11)–Ru(14)	74.8(1)
Ru(13)–P(11)–Ru(14)	111.2(1)	Ru(12)–P(12)–Ru(15)	129.8(1)
Ru(13)–P(11)–Ru(15)	82.3(1)	Ru(14)–P(11)–Ru(15)	76.2(1)
Ru(12)–P(11)–C(150)	115.1(2)	Ru(13)–P(11)–C(150)	123.9(2)
Ru(14)–P(11)–C(150)	124.5(2)	Ru(15)–P(11)–C(150)	115.1(2)
Ru(11)–P(12)–Ru(13)	76.4(1)	Ru(11)–P(12)–Ru(15)	111.6(1)
Ru(13)–P(12)–Ru(15)	82.8(1)	Ru(11)–P(12)–Ru(16)	74.5(1)
Ru(13)–P(12)–Ru(16)	130.1(1)	Ru(15)–P(12)–Ru(16)	71.6(1)
Ru(11)–P(12)–C(140)	125.1(2)	Ru(13)–P(12)–C(140)	114.8(2)
Ru(15)–P(12)–C(140)	122.9(2)	Ru(16)–P(12)–C(140)	115.1(2)

Table 4 (continued)

Ru(11)–C(11)–O(11)	172.9(5)	Ru(11)–C(12)–O(12)	174.3(6)
Ru(12)–C(13)–O(13)	176.8(6)	Ru(16)–C(12)–O(112)	178.1(6)
Ru(12)–C(14)–O(14)	176.5(5)	Ru(13)–C(15)–O(15)	177.6(6)
Ru(13)–C(16)–O(16)	176.6(5)	Ru(14)–C(17)–O(17)	176.5(5)
Ru(14)–C(18)–O(18)	176.1(6)	Ru(15)–C(19)–O(19)	172.0(6)
Ru(15)–C(110)–O(110)	178.8(6)	Ru(16)–C(111)–O(111)	176.1(7)
C(121)–C(120)–C(125)	117.9(6)	C(120)–C(121)–C(122)	121.9(7)
C(121)–C(122)–C(123)	121.2(7)	C(122)–C(123)–C(124)	120.3(7)
Ru(11)–C(124)–Ru(12)	78.7(2)	Ru(11)–C(124)–C(123)	129.1(5)
Ru(12)–C(124)–C(123)	124.1(4)	Ru(11)–C(124)–C(125)	111.9(4)
Ru(12)–C(124)–C(125)	71.5(3)	C(123)–C(124)–C(125)	118.4(6)
Ru(12)–C(125)–Ru(13)	78.9(2)	Ru(12)–C(125)–C(120)	123.5(4)
Ru(13)–C(125)–C(120)	128.9(4)	Ru(2)–C(125)–C(124)	71.5(3)
Ru(13)–C(125)–C(124)	110.2(4)	C(120)–C(125)–C(124)	120.2(5)
Ru(14)–C(130)–Ru(16)	79.0(2)	Ru(14)–C(130)–C(131)	112.1(4)
Ru(16)–C(130)–C(131)	71.8(3)	Ru(14)–C(130)–C(135)	129.1(5)
Ru(16)–C(130)–C(135)	123.9(4)	C(131)–C(130)–C(135)	118.2(6)
Ru(15)–C(131)–Ru(16)	79.3(2)	Ru(15)–C(131)–C(130)	110.2(4)
Ru(16)–C(131)–C(130)	71.0(3)	Ru(15)–C(131)–C(132)	128.8(4)
Ru(16)–C(131)–C(132)	124.9(4)	C(130)–C(131)–C(132)	120.0(5)
C(130)–C(135)–C(134)	121.0(6)	C(131)–C(132)–C(133)	118.6(7)
C(135)–C(134)–C(133)	120.2(6)	C(132)–C(133)–C(134)	122.0(7)
Ru(22)–P(21)–Ru(23)	71.5(1)	Ru(22)–P(21)–Ru(24)	73.0(1)
Ru(23)–P(21)–Ru(24)	110.1(1)	Ru(22)–P(21)–Ru(25)	129.2(1)
Ru(23)–P(21)–Ru(25)	83.1(1)	Ru(24)–P(21)–Ru(25)	75.8(1)
Ru(22)–P(21)–C(250)	116.1(2)	Ru(23)–P(21)–C(250)	124.5(2)
Ru(24)–P(21)–C(250)	125.0(2)	Ru(25)–P(21)–C(250)	114.6(2)
Ru(21)–P(22)–Ru(23)	75.8(1)	Ru(21)–P(22)–Ru(25)	112.8(1)
Ru(23)–P(22)–Ru(25)	83.2(1)	Ru(21)–P(22)–Ru(26)	76.0(1)
Ru(23)–P(22)–Ru(6)	130.3(1)	Ru(25)–P(22)–Ru(26)	71.4(1)
Ru(21)–P(22)–C(240)	123.8(2)	Ru(23)–P(22)–C(240)	114.6(2)
Ru(25)–P(22)–C(240)	123.0(2)	Ru(26)–P(22)–C(240)	115.1(2)
Ru(21)–C(21)–O(21)	174.4(5)	Ru(21)–C(22)–O(22)	178.7(6)
Ru(22)–C(23)–O(23)	176.9(7)	Ru(22)–C(24)–O(24)	179.0(6)
Ru(23)–C(25)–O(25)	176.5(6)	Ru(23)–C(26)–O(26)	175.2(6)
Ru(24)–C(27)–O(27)	177.6(5)	Ru(24)–C(28)–O(28)	174.4(6)
Ru(25)–C(29)–O(29)	172.8(5)	Ru(25)–C(210)–O(210)	177.0(5)
Ru(26)–C(211)–O(211)	176.6(7)	Ru(26)–C(212)–O(212)	175.6(6)
C(221)–C(220)–C(225)	118.7(6)	C(220)–C(221)–C(222)	122.0(7)
C(221)–C(222)–C(223)	121.9(6)	C(222)–C(223)–C(224)	118.7(5)
Ru(21)–C(224)–Ru(22)	79.5(2)	Ru(21)–C(224)–C(223)	128.8(4)
Ru(22)–C(224)–C(223)	120.8(4)	Ru(21)–C(224)–C(225)	111.9(4)
Ru(22)–C(224)–C(225)	72.5(3)	C(223)–C(224)–C(225)	118.9(5)
Ru(22)–C(225)–Ru(23)	79.0(2)	Ru(22)–C(225)–C(220)	123.1(4)
Ru(23)–C(225)–C(220)	130.0(4)	Ru(22)–C(225)–C(224)	70.2(3)
Ru(23)–C(225)–C(224)	109.8(4)	C(220)–C(225)–C(224)	119.7(5)
Ru(24)–C(230)–Ru(26)	78.5(2)	Ru(24)–C(230)–C(231)	111.7(4)
Ru(26)–C(230)–C(231)	73.4(3)	Ru(24)–C(230)–C(235)	127.5(4)
Ru(26)–C(230)–C(235)	127.3(4)	C(231)–C(230)–C(235)	119.0(5)
Ru(25)–C(231)–Ru(26)	78.3(2)	Ru(25)–C(231)–C(230)	110.3(4)
Ru(26)–C(231)–C(230)	69.7(3)	Ru(25)–C(231)–C(232)	128.3(4)
Ru(26)–C(231)–C(230)	130.2(4)	C(230)–C(231)–C(232)	119.7(5)
C(231)–C(232)–C(233)	120.4(6)	C(232)–C(233)–C(234)	119.9(7)
C(233)–C(234)–C(235)	121.6(6)	C(230)–C(235)–C(234)	119.3(6)

Table 5

μ_n-Benzyne geometries

	2a molecule (a)	**2a** molecule (b)	**2b**	**3a**	**1a**	**11** molecule (a) ring C(12*n*)	**11** molecule (a) ring C(13*n*)	**11** molecule (b) ring C(22*n*)	**11** molecule (b) ring C(23*n*)
Bonding									
mode	μ_4	μ_4	μ_4	μ_5	μ_3	μ_3	μ_3	μ_3	μ_3
C^1–Ru (σ)	2.108(10)	2.100(11)	2.115(4)	2.097(6)	2.135(6)	2.105(6)	2.097(6)	2.098(6)	2.102(6)
C^2–Ru (σ)	2.110(10)	2.122(10)	2.117(3)	2.116(6)	2.127(6)	2.091(6)	2.096(6)	2.087(6)	2.095(6)
C^1–Ru (π)	2.294(9)	2.309(12)	2.301(4)	2.234(5)	2.353(6)	2.216(6)	2.198(5)	2.188(5)	2.195(5)
C^2–Ru (π)	2.299(10)	2.317(13)	2.292(4)	2.251(6)	–	–	–	–	–
C^3–Ru (π)	2.689(11)	2.619(14)	2.592(4)	2.390(6)	–	–	–	–	–
C^4–Ru (π)	–	–	–	2.427(6)	–	–	–	–	–
C^5–Ru (π)	–	–	–	2.398(7)	–	–	–	–	–
C^6–Ru (π)	2.656(11)	2.583(12)	2.634(4)	2.391(5)	2.303(6)	2.215(6)	2.208(5)	2.217(5)	2.241(5)
C^1–C^2	1.455(15)	1.460(16)	1.447(5)	1.451(9)	1.400	1.409(8)	1.404(8)	1.406(7)	1.404(7)
C^2–C^3	1.395(14)	1.419(18)	1.391(5)	1.395(9)	1.410	1.436(9)	1.426(10)	1.444(9)	1.400(9)
C^3–C^4	1.399(18)	1.394(20)	1.427(6)	1.441(10)	1.355	1.363(10)	1.350(9)	1.355(9)	1.360(10)
C^4–C^5	1.360(20)	1.355(25)	1.344(6)	1.394(10)	1.391	1.395(11)	1.410(11)	1.382(9)	1.418(10)
C^5–C^6	1.405(16)	1.373(20)	1.407(6)	1.443(10)	(1.355)	1.339(11)	1.329(10)	1.364(10)	1.334(10)
C^1–C^6	1.403(16)	1.393(14)	1.402(6)	1.380(9)	(1.410)	1.427(9)	1.431(8)	1.450(8)	1.439(8)
Interplanar									
angle C_6: Ru_n	54.7	49.0	50.9	41.8	65.2	68.9	68.6	64.4	73.4

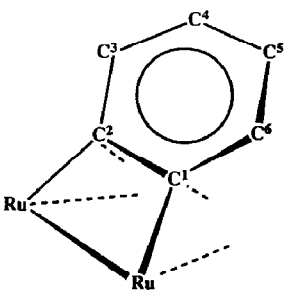

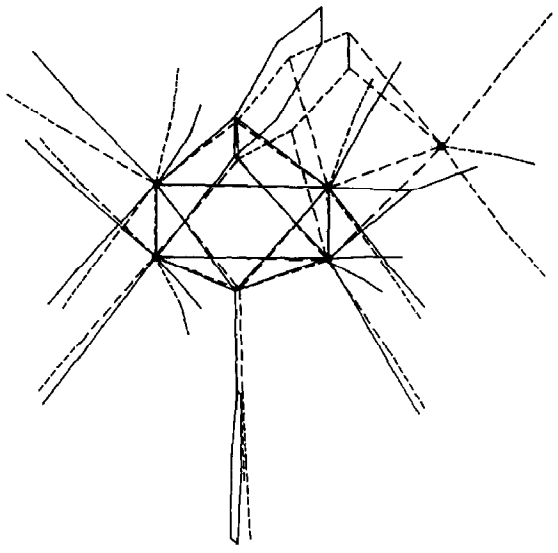

Fig. 5. Comparison of the non-hydrogen atom geometries of **2a** and **3a**, superimposed by least-squares fit of their Ru_4 units.

Ru_4 complex **4** [20], in which the Ru–C(π) interactions are apparently fully cleaved. Furthermore, the "softness" of this angle is consistent with the ease of benzyne "rotation" noted from the NMR spectroscopic studies of **2a** discussed above. The larger (> 60°) interplanar angles reported here are associated with the μ_3-benzyne ligands, and the smallest value with the μ_5-benzyne of **3a**. As illustrated in Fig. 5 the presence of a third η^2-interaction pulls the benzyne down closer to the Ru_4 plane. The benzyne ligands may be described as *ortho*-dimetallated benzenes which are further involved in one, two or three η^2 interactions with other ruthenium atoms. The influence of these interactions on the aromaticity of the C_6 ring is clear. The μ_4-benzyne ligands of **2a** and **2b** have shortened C^4–C^5 and lengthened C^1–C^2 distances, while the μ_5-benzyne of **3a** has C^1–C^2, C^3–C^4 and C^5–C^6 all ca. 0.06 Å longer than the η^2-coordinated C–C bonds. In the μ_3-benzyne ligands of **1a** [8] and **11** the C^3–C^4 and C^5–C^6 bonds are short, and C^1–C^6, C^2–C^3 and (to a lesser extent) C^4–C^5 are longer. The implication is that the η^2-bonding localises the π-electrons of the C_6 rings. This produces alternating long and short C–C distances, approaching those that might be expected in a cyclohexatriene, albeit with the η^2-bound C–C "double" bond lengths being ca 1.4 Å rather than ca 1.33 Å as a consequence of the effects of coordination. Similar disturbance of C–C bond lengths from equality in co-ordinated aromatic systems has been noted in non-cluster chemistry [27].

There has been a report of the structure of an isoelectronic, 88-electron, cluster with closely related geometry to that of **11**. The complex $[Ru_6(CO)_{12}(\mu_3\text{-PPh})_2(\mu_4\text{-PPh})_2]$ has a structure formally derived from that of **11** by replacement of the four-electron donor μ_3-benzyne ligands with four-electron μ_3-PPh groups. The resulting Ru_6 core geometry is essentially identical to that in **11**, differing principally only in a marked lengthening of the diagonal Ru–Ru distance [Ru(11)–Ru(14) in **11**] to ca. 3.25 Å [21].

Experimental

Reactions were performed under dinitrogen by standard Schlenk procedures. Toluene (sodium), hexane (sodium), tetrahydrofuran (sodium/benzophenone), dichloromethane (calcium hydride) were dried by distillation over the drying agent indicated. Chromatography was performed either on alumina (Brockman activity II) or Florisil columns (ca 3 × 30 cm). Infrared spectra were recorded on a Perkin-Elmer FT1710 spectrophotometer, ^{31}P NMR spectra with JEOL FX 90Q and a JEOL GX 400 spectrometers, and ^{1}H and ^{13}C NMR spectra with JEOL GX 270 and 400 spectrometers. Mass spectra were recorded with an EI MS 912 spectrometer; FAB spectra were supplied by the SERC Mass Spectroscopy Service at Swansea. Complexes $[Ru_3(CO)_{11}(ER_2)]$ (E = P, As) and $[Ru_3(CO)_{10}(PR_3)_2]$ were prepared by literature methods [28].

Thermolysis of $[Ru_3(CO)_{11}(PPh_2CH_2NPh_2)]$

$[Ru_3(CO)_{11}(PPh_2CH_2NPh_2)]$ (0.35 g, 0.36 mmol) was refluxed in toluene (100 cm^3) for 18 h. The solvent was removed under reduced pressure and the residue chromatographed on alumina. Elution with hexane : dichloromethane (6 : 1) developed several bands. The first yielded a trace of $[Ru_3(CO)_{12}]$. The second contained a mixture of several compounds and was chromatographed again, yielding 25 mg (9%) of pure **2b** [ν(CO) (in hexane): 2083w, 2051m, 2039s, 2021m, 1992m, 1978w, and 1826w cm^{-1}. ^{1}H NMR (in $CDCl_3$): δ 7.27 (m, 4H), 7.00 (m, 8H), 6.44 (m, 2H), and 5.46 (d, J 6 Hz, 2H). ^{31}P{^{1}H} NMR (in $CDCl_3$): δ 415.0s. ^{13}C{^{1}H} NMR {in $(CD_3)_2CO$}: δ 200.7 (d, J 12 Hz), 148.6s, 144.5 (d, J 3 Hz), 129.5s, 129.2s, 127.0 (d, J 4 Hz), 123.5s, 122.7s, and 63.9 (d, J 10Hz). Found: C, 35.9; H 1.7, N 1.3%; $Ru_4C_{31}H_{16}O_{11}PN$ requires: C 36.0, H 1.6, N 1.4%].

Thermolysis of $[Ru_3(CO)_{11}(PPh_3)]$

$[Ru_3(CO)_{11}(PPh_3)]$ (0.35 g, 0.40 mmol) was refluxed in toluene (100 cm^3) for 18 h. The solvent was removed under reduced pressure and the residue chromatographed on alumina. Elution with hexane : dichloromethane (6 : 1) developed four bands. The first yielded a trace of $[Ru_3(CO)_{12}]$. The second gave 60 mg (33%) of purple, crystalline $[Ru_3(CO)_7(PPh_2)_2(C_6H_4)]$ (**1a**) [ν(CO) (in hexane): 2057m, 2020m, 2010s, 1999m, 1969m, and 1955mw cm^{-1}. ^{1}H NMR {in $(CD_3)_2CO$ at 25 °C}: δ 7.77–7.69 (m, 4H), 7.49–7.30 (m, 16H), 6.90 (br, 2H), and 6.45(br, 2H). ^{31}P{^{1}H} NMR (in $CDCl_3$): δ 239.6. ^{13}C{^{1}H} NMR {in $(CD_3)_2CO$}: δ 143.3 (t, J 15 Hz), 140.5 (t, J 15 Hz), 132.8 (t, J 6 Hz), 132.5 (t, J 6 Hz), 131.0s, 130.1s, 128.7 (t, J 5 Hz), 128.3 (t, J 5 Hz), and 125.7s. Found: C 46.88, H 2.58%; $Ru_3C_{37}H_{24}O_7P_2$ requires: C 46.98, H 2.56%]. The third band gave 132 mg (49%) of red crystalline $[Ru_4(CO)_{11}(\mu_4\text{-PPh})(\mu_4\text{-}\eta^4\text{-}C_6H_4)]$ (**2a**) [ν(CO) (in hexane): 2083w, 2049s, 2042vs, 2027m, 2023s, 1997mw, 1987w, and 1826mw cm^{-1}. ^{1}H NMR {in $(CD_3)_2CO$}: δ 6.65 (m, 2H), 7.15 (m, 2H), 7.55 (m, 3H), and 7.75 (m, 2H); ^{31}P{^{1}H} NMR (in $CDCl_3$): δ 411.6. ^{13}C{^{1}H} NMR {in $(CD_3)_2CO$}: δ 200.4 br, 144.5 (d, J 5 Hz), 141.8 (d, J 22 Hz), 133.0 (d, J 14 Hz), 132.0s, 128.7s, 128.1 (d, J 10 Hz), and 121.0 (d, J 5 Hz). Found: C, 30.7; H, 1.0%; M 898; $Ru_4C_{23}H_9O_{11}P$ requires: C, 30.8; H, 1.0%; M, 898]. The fourth band gave 16 mg (6%) of red crystalline $[Ru_5(CO)_{13}(\mu_4\text{-PPh})(\mu_5\text{-}\eta^6\text{-}C_6H_4)]$ (**3a**) [ν(CO) (in hexane): 2060vs, 2049m, 2025m, 2018mw, and 2013s cm^{-1}. ^{1}H NMR {in $(CD_3)_2CO$): δ 5.49 (m,2 H), 5.83 (m, 2H), and 7.45–7.49

(m, 5H). $^{31}P\{^1H\}$ NMR (in $CDCl_3$): δ 423.7s. $^{13}C\{^1H\}$ NMR {in $(CD_3)_2CO$}: δ 153.8 (d, J 8Hz), 143.1 (d, J 22 Hz), 134.1 (d, J 14 Hz), 132.2 (d, J 2 Hz), 128.0 (d, J 12 Hz), 89.4 (d, J 3 Hz), and 71.8s ppm. Found: C, 28.5, H 0.9%; $Ru_5C_{25}H_9O_{13}P$ requires: C 28.5, H 0.9%]. A fifth band, eluted with hexane : dichloromethane (3 : 2), yielded a few milligrammes of a mixture that was not characterized.

Thermolysis of $[Ru_3(CO)_{10}(PPh_3)_2]$

A solution of $[Ru_3(CO)_{10}(PPh_3)_2]$ (0.35 g, 0.32 mmol) in toluene (100 cm^3) was refluxed for 2.5 h. The solvent was removed under reduced pressure and the residue chromatographed on alumina. Elution with hexane : dichloromethane (6 : 1) developed two bands. The first gave 180 mg (59%) of **1a**. The second, eluted with hexane : dichloromethane (7 : 3), gave a few milligrammes of a complex mixture that was not characterized.

Thermolysis of $[Ru_3(CO)_{11}(PR_3)]$ (R = m-tolyl or p-tolyl)

Solutions of each of the complexes $[Ru_3(CO)_{11}(PR_3)]$ (R = *m*-tolyl or *p*-tolyl) (0.35 g, 0.38 mmol) in toluene (100 cm^3) were refluxed for 2.5 h. The solvent was removed under reduced pressure and the residue chromatographed on alumina. Elution with hexane : dichloromethane (20 : 1) developed three bands. The first yielded a trace of $[Ru_3(CO)_{12}]$. The second, purple band gave ca 4 mg (10%) of the corresponding known [7] $[Ru_3(CO)_7(\mu\text{-}PR_2)_2(\mu_3\text{-}\eta^2\text{-}C_6H_3\text{-}4\text{-}Me)]$ complex **1b** or **1c**, identified by IR and ^1H NMR spectra. The third, red band gave ca 140 mg (40%) of $[Ru_4(CO)_{11}(\mu_4\text{-}PR)(\mu_4\text{-}\eta^4\text{-}C_6H_3\text{-}4\text{-}Me)]$ (**2c** or **2d**) [**2c**, ν(CO) (in hexane): 2082m, 2048s, 2040vs, 2025s, 2021s, 1995m, 1985m, 1978w, and 1822w cm^{-1}. ^1H NMR {in $(CD_3)_2CO$}: δ 7.3–7.6 (m, 4H), 6.89 (d, J 6 Hz, 1H), 6.61 (d, J 6 Hz, 1H), 6.40 (d, J 2 Hz, 2H), 2.39 (s, 3H), and 2.18 (d, J 1 Hz, 3H). $^{31}P\{^1H\}$ NMR (in $CDCl_3$): δ 411.0s. Found: C 32.3, H 1.4%; $Ru_4C_{35}H_{13}O_{11}P$ requires: C 32.5, H 1.4%. **2d**, ν(CO) (in hexane): 2082m, 2048s, 2040vs, 2025s, 2021s, 1995m, 1985m, 1978w, and 1822w cm^{-1}. ^1H NMR {in $(CD_3)_2CO$}: δ 7.58 (dd, J 14 Hz, 4 Hz, 2H), 7.36 (d, J 9 Hz, 2H), 6.88 (d, J 6 Hz, 1H), 6.60 (d, J 6 Hz, 1H), 6.39 (d, J 2 Hz, 1H), 2.39 (s, 3H), and 2.18 (d, J 1 Hz, 3H). $^{31}P\{^1H\}$ NMR (in $CDCl_3$): δ 410.6. $^{13}C\{^1H\}$ NMR {in $(CD_3)_2CO$}: δ 201.3 br, 145.6 (d, J 7 Hz), 143.3 (d, J 2 Hz), 140.5s, 139.7 (d, J 4 Hz), 139.6s, 139.4s, 133.5 (d, J 14 Hz), 129.1 (d, J 4 Hz), 120.3 (d, J 5 Hz), 20.7s, and 20.3s. Found: C 33.6, H 1.8%; $Ru_4C_{35}H_{13}O_{11}P$ requires: C 32.5, H 1.4%].

Thermolysis of $[Ru_3(CO)_{11}(PPh_2Me)]$

A solution of $[Ru_3(CO)_{11}(PPh_2Me)]$(0.635 g, 0.78 mmol) in octane (100 cm^3) was refluxed for 2.5 h. The solvent was removed under reduced pressure and the residue chromatographed on Florisil. Elution with hexane developed three bands. The first yielded 150 mg of $[Ru_3(CO)_{12}]$. The second gave 45 mg (10%) of dark green $[Ru_5(CO)_{15}(\mu_4\text{-}PMe)]$ (**10a**) [24], identified by IR, $^{31}P\{^1H\}$ and ^1H NMR spectra. The third band gave 52 mg (11%) of dark purple crystalline $[Ru_6(CO)_{12}(\mu_4\text{-}PMe)_2(\mu_3\text{-}\eta^2\text{-}C_6H_4)_2]$ (**11**) [ν(CO) (in hexane): 2061w, 2034vs, 2025s, 2018m, 2006w, 1986w, and 1961vw cm^{-1}. ^1H NMR {in $(CD_3)_2CO$}: δ 8.32 (d, J 9 Hz, 2H), 8.05 (d, J 9 Hz, 2H), 7.16 (m, 4H), and 3.46 (d, J 9 Hz, 6H). $^{31}P\{^1H\}$ NMR (in $CDCl_3$) δ 520.9. Found: C 26.3, H 1.2%, M 1188, $Ru_6C_{26}H_{14}O_{12}P_2$ requires: C 26.3, H 1.2%, M 1188].

Table 6

Details of structure analyses

	2a	2b	3a	11
Crystal data				
Formula	$C_{23}H_9O_{11}PRu_4$	$C_{30}H_{16}NO_{11}PRu_4$	$C_{25}H_9O_{13}PRu_5$	$C_{26}H_{14}O_{12}P_2Ru_6$
M	896.6	1001.7	1053.7	1186.8
Crystal system	triclinic	monoclinic	monoclinic	triclinic
Space group (No.)	$P\bar{1}$ (No. 2)	$P2_1/n$ (No. 14)	$P2_1/n$ (No. 14)	$P\bar{1}$ (No. 2)
a (Å)	9.326(2)	9.650(2)	10.037(2)	10.233(2)
b	15.884(3)	19.571(5)	18.311(3)	17.090(3)
c	18.796(4)	17.558(4)	16.425(2)	19.213(3)
α (°)	88.80(2)	90	90	81.83(2)
β	77.37(2)	101.47(2)	102.20(1)	84.28(2)
γ	88.64(2)	90	90	87.64(2)
U (Å^3)	2715.8(7)	3249.8(13)	2950.5(7)	3307.9(9)
T (K)	295	295	295	295
Z	4	4	4	4
D_c (g cm^{-3})	2.19	2.05	2.37	2.38
F(000)	1704	1920	1992	2240
μ(Mo-K_α cm^{-1})	22.6	19.0	25.7	27.8
Data collection and reduction				
Crystal dimensions (mm)	0.015×0.2×0.2	0.35×0.35×0.5	0.075×0.3×0.4	0.31×0.42×0.7
Scan width (ω°)	$1.1+\Delta\alpha_1\alpha_2$	$1.2+\Delta\alpha_1\alpha_2$	$1.1+\Delta\alpha_1\alpha_2$	$1.3+\Delta\alpha_1\alpha_2$

Total data	7389	6484	5288	13214
Unique data	6600	5717	4355	11647
"Observed" data (N.O.)	4992	5040	3873	10300
Observation criterion $[F^2 > n\,\sigma(F^2)]$	1.5	1.5	1.5	1.5
Crystal faces [distance from origin (mm)]	(001)[.0075],(1̄10)[0.1], (00$\bar{1}$)[.0075],(1$\bar{1}$0)[0.1], (012)[0.1],(0$\bar{1}$2̄)[0.1]	(010)[0.15], (0$\bar{1}$0)[0.15], (011)[0.15], (0$\bar{1}\bar{1}$)[0.15], (10$\bar{1}$)[0.316], (1̄01)[0.316], (001)[0.095], (00$\bar{1}$)[0.095], (021)[0.16), (01$\bar{1}$)[0.15], (0$\bar{1}$1)[0.125]	–	–
No. azimuthal scan data used	–	–	362	628
Min., max. transmission coef.	0.626,0.969	0.572,0.718	0.435,0.849	0.112,0.183
Refinement				
Anisotropic atoms	All non-H, except C(1–11)	All non-H	All non-H	All non-H
Least squares variables (N.V.)	593	488	409	844
R [a]	0.050	0.029	0.034	0.030
wR [a]	0.042	0.035	0.040	0.047
S [a]	1.17	1.18	1.14	1.33
g	0.0002	0.0003	0.0005	0.0008
Final difference map features (e Å^{-3})	+0.9, −0.7	+0.56, −0.39	+0.55, −0.54	+0.48, −0.73

[a] $R = \Sigma|\Delta|/\Sigma|F_o|$; $wR = [\Sigma w\Delta^2/\Sigma wF_o^2]^{1/2}$; $S = [\Sigma w\Delta^2/(\text{N.O.} - \text{N.V.})]^{1/2}$; $\Delta = F_o - F_c$; $w = [\sigma_c^2(F_o) + gF_o^2]^{-1}$, $\sigma_c^2(F_o)$ = variance in F_o due to counting statistics.

Table 7

Atomic coordinates ($\times 10^4$) and isotropic thermal parameters ($Å^2 \times 10^3$) for **2a**

	x	y	z	U
Ru(1a)	5684(1)	1602(1)	3997(1)	32(1)*
Ru(2a)	8446(1	1477(1)	4511(1)	31(1)*
Ru(3a)	9035(1)	3193(1)	3998(1)	33(1)*
Ru(4a)	6403(1)	3313(1)	3522(1)	33(1)*
P(1a)	8030(3)	2069(2)	3414(2)	29(1)*
O(1a)	3060(8)	2179(5)	3395(5)	69(4)*
O(2a)	3810(9)	817(5)	5375(4)	62(4)*
O(3a)	6077(9)	45(5)	3040(5)	67(4)*
O(4a)	6870(9)	583(6)	5893(5)	72(4)*
O(5a)	9892(11)	−164(5)	3829(5)	84(4)*
O(6a)	11142(9)	1887(5)	5086(5)	69(4)*
O(7a)	11073(10)	4067(6)	4788(5)	84(5)*
O(8a)	11232(9)	3578(6)	2615(5)	71(4)*
O(9a)	7444(11)	3809(6)	1948(4)	82(4)*
O(10a)	3694(8)	4348(5)	3381(5)	65(4)*
O(11a)	7761(8)	4933(4)	3856(5)	54(3)*
C(1a)	4088(12)	2012(7)	3612(6)	43(3)
C(2a)	4496(11)	1082(7)	4864(6)	39(3)
C(3a)	5940(12)	605(7)	3393(6)	47(3)
C(4a)	7447(12)	911(7)	5378(6)	44(3)
C(5a)	9364(12)	436(7)	4054(6)	45(3)
C(6a)	10164(12)	1750(7)	4851(6)	45(3)
C(7a)	10295(13)	3736(7)	4508(7)	52(3)
C(8a)	10398(12)	3425(7)	3120(6)	44(3)
C(9a)	7084(12)	3609(7)	2542(6)	44(3)
C(10a)	4698(12)	3956(7)	3456(6)	42(3)
C(11a)	7722(12)	4202(7)	3809(6)	43(3)
C(15a)	8921(10)	1723(6)	2503(5)	27(4)*
C(16a)	10396(12)	1485(7)	2347(7)	51(5)*
C(17a)	11013(13)	1204(9)	1649(7)	69(6)*
C(18a)	10222(15)	1180(9)	1125(7)	74(6)*
C(19a)	8765(14)	1425(8)	1287(7)	64(6)*
C(20a)	8125(13)	1683(8)	1983(6)	59(5)*
C(25a)	7253(10)	2587(7)	4884(5)	30(4)*
C(26a)	5873(10)	2645(6)	4643(6)	33(4)*
C(27a)	4896(12)	3299(7)	4916(6)	44(5)*
C(28a)	5210(14)	3907(7)	5385(7)	54(5)*
C(29a)	6496(15)	3846(7)	5613(7)	60(6)*
C(30a)	7518(13)	3193(7)	5370(6)	46(5)*
Ru(1b)	4768(1)	6411(1)	1494(1)	49(1)*
Ru(2b)	4366(1)	8160(1)	1980(1)	38(1)*
Ru(3b)	1419(1)	8162(1)	1688(1)	42(1)*
Ru(4b)	1809(1)	6487(1)	1227(1)	49(1)*
P(1b)	3698(3)	7549(2)	973(2)	39(1)*
O(1b)	4263(14)	4608(7)	1151(9)	160(8)*
O(2b)	6354(11)	5914(6)	2711(5)	96(5)*
O(3b)	7598(10)	6531(8)	306(6)	117(6)*
O(4b)	5764(12)	7845(6)	3294(6)	100(5)*
O(5b)	7166(9)	8882(6)	998(6)	94(5)*
O(6b)	3082(9)	9872(5)	2496(5)	61(4)*
O(7b)	−960(12)	9337(7)	2510(6)	113(6)*
O(8b)	821(11)	9144(6)	396(5)	85(5)*
O(9b)	1340(11)	6636(7)	−300(5)	97(5)*

Table 7 (continued)

O(10b)	351(17)	4799(7)	1276(8)	168(9)*
O(11b)	−1320(9)	7193(6)	1678(5)	83(4)*
C(1b)	4411(17)	5308(10)	1263(9)	97(5)
C(2b)	5751(15)	6096(8)	2265(7)	69(4)
C(3b)	6574(14)	6469(8)	747(7)	66(4)
C(4b)	5257(13)	7949(8)	2800(7)	57(4)
C(5b)	6124(14)	8625(8)	1358(7)	64(4)
C(6b)	3499(12)	9218(7)	2299(6)	45(3)
C(7b)	−55(15)	8892(8)	2231(8)	70(4)
C(8b)	1043(13)	8747(7)	861(7)	52(3)
C(9b)	1542(14)	6569(8)	282(7)	65(4)
C(10b)	936(17)	5415(10)	1274(9)	92(5)
C(11b)	−44(14)	7236(8)	1573(7)	59(4)
C(15b)	4330(11)	7901(7)	35(6)	38(4)*
C(16b)	4374(12)	8753(7)	−149(7)	43(5)*
C(17b)	4837(13)	9022(8)	−863(8)	59(6)*
C(18b)	5263(14)	8435(9)	−1408(7)	61(6)*
C(19b)	5219(14)	7592(9)	−1235(8)	62(6)*
C(20b)	4757(13)	7341(7)	−528(7)	49(5)*
C(25b)	2540(11)	7435(7)	2502(6)	39(4)*
C(26b)	2773(13)	6565(7)	2259(6)	50(5)*
C(27b)	1680(16)	5979(8)	2574(8)	67(6)*
C(28b)	411(17)	6245(11)	3064(8)	81(8)*
C(29b)	210(16)	7059(11)	3271(8)	84(7)*
C(30b)	1267(13)	7644(8)	3014(6)	55(5)*

* Equivalent isotropic U defined as one-third of the trace of the orthogonalised U_{ij} tensor.

Thermolysis of $[Ru_3(CO)_{11}(AsPh_3)]$

A solution of $[Ru_3(CO)_{11}(AsPh_3)]$ (0.15 g, 0.16 mmol) in toluene (110 cm^3) was refluxed for 1 h. The solvent was then removed under reduced pressure and the resulting brown oil transferred to a Florisil column. Elution with hexane gave three bands. The first afforded 7 mg (7%) of green $[Ru_5(CO)_{15}(\mu_4\text{-AsPh})]$ (**10b**), identified by IR [ν(CO) (in hexane): 2056vs, 2032s, and 1993w cm^{-1}]. The second gave 44 mg (65%) of yellow crystalline $[Ru_2(CO)_6(\mu\text{-AsPh}_2)_2]$ (**12**) [ν(CO) (in hexane): 2076s, 2045vs, 2011s, 2001s, and 1981s cm^{-1}. ^{1}H NMR (in CD_2Cl_2) δ 7.1–7.7m. Found: C 43.4, H 2.4%; $Ru_2C_{30}H_{20}As_2O_6$ requires: C 43.5, H 2.5%]. The third provided 16 mg of a blue mixture of **12** and an unidentified product. Subsequent elution with hexane : diethylether (50 : 1) gave an orange band which yielded 6 mg (6%) of maroon crystalline $[Ru_4(CO)_{11}(\mu_4\text{-AsPh})(\mu_4\text{-}\eta^4\text{-}C_6H_4)]$ (**2e**) [ν(CO) (in hexane): 2081w, 2047s, 2040vs, 2023s, 1995m, 1986w, and 1826w cm^{-1}. ^{1}H NMR (in CD_2Cl_2): δ 7.5–7.7 (m, 5H), 6.99 (m, 2H), and 6.42 (m, 2H). Found: C 29.4, H 1.2%; M 942; $Ru_4C_{23}H_9AsO_{11}$ requires: C 29.3, H 1.0%, M 942]. Final elution with hexane : diethylether (30 : 1) separated an orange band which contained 5 mg (5%) of red crystalline $[Ru_5(CO)_{13}(\mu_4\text{-AsPh})(\mu_5\text{-}\eta^6\text{-}C_6H_4)]$ (**3b**) [ν(CO) (in hexane): 2060s, 2047m, 2022m, and 2011m cm^{-1}. ^{1}H NMR (in $CDCl_3$): δ 7.4–8.0 (m, 5H) and 5.1–5.5 (m, 4H)].

*Crystal structure determinations for **2a, 2b, 3a and 11***

Many of the details of the structure analyses carried out on **2a**, **2b**, **3a** and **11** are listed in Table 6. X-ray diffraction measurements were made using Nicolet four-circle

Table 8

Atomic coordinates ($\times 10^4$) and isotropic thermal parameters ($Å^2 \times 10^3$) for **2b**

	x	*y*	*z*	*U*
Ru(1)	8130(1)	3651(1)	9914(1)	33(1)*
Ru(2)	6317(1)	2828(1)	8730(1)	32(1)*
Ru(3)	8712(1)	2677(1)	7949(1)	32(1)*
Ru(4)	10442(1)	3438(1)	9130(1)	30(1)*
P	7943(1)	3683(1)	8554(1)	29(1)*
N	6984(3)	4454(2)	7192(2)	37(1)*
O(1)	10678(4)	4229(2)	11025(2)	79(2)*
O(2)	6737(4)	3043(2)	11179(2)	88(2)*
O(3)	6487(4)	4997(2)	9858(3)	82(2)*
O(4)	4985(5)	1999(2)	9874(3)	85(2)*
O(5)	3949(3)	3901(2)	8502(2)	63(1)*
O(6)	5070(4)	1941(2)	7347(2)	79(2)*
O(7)	8598(5)	1388(2)	6973(2)	87(2)*
O(8)	8944(4)	3388(2)	6461(2)	64(1)*
O(9)	11301(3)	4699(2)	8369(2)	54(1)*
O(10)	13370(3)	3433(2)	10138(2)	62(1)*
O(11)	11888(3)	2545(2)	8112(2)	59(1)*
C(1)	9776(5)	4012(2)	10581(3)	51(2)*
C(2)	7260(5)	3264(3)	10713(3)	54(2)*
C(3)	7089(5)	4505(2)	9887(2)	48(1)*
C(4)	5486(5)	2309(2)	9456(3)	50(2)*
C(5)	4781(4)	3493(2)	8545(2)	44(1)*
C(6)	5599(5)	2267(2)	7856(3)	50(2)*
C(7)	8623(5)	1862(2)	7348(3)	49(2)*
C(8)	8826(4)	3143(2)	7033(2)	42(1)*
C(9)	10976(4)	4211(2)	8640(2)	37(1)*
C(10)	12271(4)	3437(2)	9780(2)	40(1)*
C(11)	10887(4)	2772(2)	8297(2)	38(1)*
C(12)	7457(4)	4505(2)	8024(2)	36(1)*
C(13)	7512(4)	4812(2)	6649(2)	36(1)*
C(14)	6851(5)	4796(2)	5862(2)	48(1)*
C(15)	7452(6)	5104(2)	5306(3)	58(2)*
C(16)	8726(5)	5444(2)	5497(3)	59(2)*
C(17)	9349(5)	5485(2)	6266(3)	58(2)*
C(18)	8770(4)	5178(2)	6844(3)	49(1)*
C(19)	5393(4)	4344(2)	6995(2)	40(1)*
C(20)	4481(5)	4865(2)	7102(3)	53(2)*
C(21)	3042(5)	4771(4)	6908(3)	75(2)*
C(22)	2504(5)	4158(4)	6608(3)	94(3)*
C(23)	3401(6)	3648(3)	6494(3)	83(2)*
C924)	4849(5)	3739(2)	6682(3)	54(2)*
C(25)	8260(4)	2315(2)	9122(2)	32(1)*
C(26)	9118(4)	2718(2)	9729(2)	32(1)*
C(27)	10406(4)	2445(2)	10103(2)	38(1)*
C(28)	10902(5)	1802(2)	9883(3)	43(1)*
C(29)	10088(4)	1430(2)	9324(3)	44(1)*
C(30)	8751(4)	1670(2)	8949(2)	38(1)*
H(1)	8224(37)	4752(19)	8132(20)	35(10)
H(2)	6848(40)	4710(21)	8284(22)	45(11)
H(3)	6026(43)	4648(22)	5736(24)	58(13)
H(4)	7085(45)	5091(23)	4800(25)	62(13)
H(5)	9131(54)	5565(26)	5060(31)	93(17)
H(6)	10142(38)	5718(19)	6451(21)	36(10)

Table 8 (continued)

	x	y	z	U
H(7)	9264(44)	5219(23)	7360(25)	57(13)
H(8)	4792(45)	5252(23)	7282(25)	60(13)
H(9)	2372(57)	5174(33)	6941(32)	107(20)
H(10)	1654(69)	3971(37)	6534(39)	139(24)
H(11)	3180(58)	3285(29)	6373(30)	91(18)
H(12)	5453(40)	3417(20)	6598(22)	40(11)
H(13)	10912(34)	2632(16)	10524(18)	24(8)
H(14)	11762(49)	1646(24)	10154(26)	60(14)
H(15)	10451(43)	1016(22)	9180(24)	60(13)
H(16)	8112(38)	1407(19)	8635(21)	26(9)

* Equivalent isotropic U defined as one-third of the trace of the orthogonalised U_{ij} tensor.

P3m diffractometers on single crystals mounted in thin-walled glass capillaries at room temperature using graphite monochromated Mo-K_α X-radiation ($\bar{\lambda} = 0.71069$ Å). Cell dimensions for each analysis were determined from the setting angle values of 25, 25, 25 and 33 centred reflections, respectively.

For each structure analysis, intensity data were collected for unique portions of reciprocal space for $4 < 2\theta < 50°$ and corrected for Lorentz, polarisation, crystal decay (negligible in each case) and long-term intensity fluctuations, on the basis of the intensities of three check reflections repeatedly measured during data collection. For **2a** and **3a** only reflections with intensity above a low threshold were recorded for $40 < 2\theta < 50°$. Corrections for X-ray absorption effects were applied for **2a** and **2b** on the basis of the indexed crystal faces and dimensions, and for **3a** and **11** by an empirical correction derived from azimuthal scan data. The structures were solved by heavy atom (Patterson or direct, and difference Fourier) methods, and refined by blocked-cascade least-squares against F. In each of **2a** and **11** there are two crystallographically distinct molecules present.

All hydrogen atoms in **2a**, **3a** and **11** were constrained to ideal geometries (with C–H = 0.96 Å), except for the benzyne hydrogens of **3a**. All other atoms were refined without positional constraints. All hydrogen atoms were assigned isotropic displacement parameters which were fixed for **2a** and **3a**; for **11** each set of benzyne and methyl group hydrogens were assigned common refined isotropic U_{iso}.

Final difference syntheses showed no chemically significant features, the largest typically being close to the metal atoms. Refinements converged smoothly to residuals given in Table 6. Tables 7–10 report the positional parameters for these structure determinations. Full tables of interatomic distances and bond angles, displacement parameters, hydrogen atomic parameters and observed and calculated structure amplitudes are given in supplementary material. All calculations were made with programs of the SHELXTL [29] system as implemented on a Nicolet structure determination system. Complex neutral-atom scattering factors were taken from ref. 30.

Table 9

Atomic coordinates ($\times 10^4$) and isotropic thermal parameters ($Å^2 \times 10^3$) for **3a**

	x	*y*	*z*	*U*
Ru(1)	9655(1)	3915(1)	7480(1)	37(1)*
Ru(2)	12125(1)	3122(1)	7393(1)	38(1)*
Ru(3)	11630(1)	2143(1)	8688(1)	33(1)*
Ru(4)	9180(1)	2920(1)	8760(1)	30(1)*
Ru(5)	9335(1)	1409(1)	8936(1)	42(1)*
P	11299(2)	3429(1)	8609(1)	30(1)*
O(1)	6715(6)	4346(4)	7399(4)	96(3)*
O(2)	9415(8)	4167(4)	5624(3)	97(3)*
O(3)	10706(8)	5469(3)	7961(4)	106(3)*
O(4)	11616(7)	2946(4)	5507(3)	113(4)*
O(5)	13780(5)	4553(3)	7606(4)	77(2)*
O(6)	14592(5)	2136(3)	7590(4)	80(3)*
O(7)	13488(6)	833(4)	8696(4)	84(3)*
O(8)	12855(6)	2324(3)	10516(3)	75(2)*
O(9)	9874(6)	3314(3)	10584(3)	73(2)*
O(10)	6276(5)	3245(4)	8885(4)	83(3)*
O(11)	6597(7)	818(5)	9114(5)	115(4)*
O(12)	10080(7)	1676(3)	10786(3)	82(3)*
O(13)	10756(7)	−58(3)	9178(4)	91(3)*
C(1)	7812(7)	4167(4)	7459(5)	58(3)*
C(2)	9538(9)	4071(4)	6320(4)	65(3)*
C(3)	10324(8)	4894(4)	7778(4)	57(3)*
C(4)	11800(8)	3036(5)	6210(4)	68(3)*
C(5)	13229(7)	4008(4)	7517(4)	54(3)*
C(6)	13646(7)	2478(5)	7541(5)	58(3)*
C(7)	12782(7)	1315(4)	8682(4)	52(3)*
C(8)	12386(7)	2245(4)	9826(4)	49(3)*
C(9)	9621(7)	3147(4)	9906(4)	44(2)*
C(10)	7356(7)	3127(4)	8813(4)	51(3)*
C(11)	7601(9)	1046(5)	9032(5)	70(3)*
C(12)	9822(8)	1612(4)	10073(4)	54(3)*
C(13)	10199(9)	485(4)	9061(4)	62(3)*
C(15)	12261(6)	3989(4)	9440(4)	36(2)*
C(16)	13636(6)	3853(4)	9742(4)	43(2)*
C(17)	14367(7)	4272(4)	10394(4)	53(3)*
C(18)	13721(8)	4824(4)	10731(4)	58(3)*
C(19)	12364(8)	4963(4)	10425(4)	56(3)*
C(20)	11639(7)	4549(4)	9786(4)	44(2)*
C(25)	10518(6)	2373(4)	7386(3)	35(2)*
C(26)	9295(6)	2786(3)	7415(3)	35(2)*
C(27)	8106(6)	2404(3)	7450(4)	36(2)*
C(28)	8117(7)	1619(4)	7514(4)	47(2)*
C(29)	9302(8)	1232(4)	7485(4)	48(2)*
C(30)	10513(6)	1619(4)	7390(3)	39(2)*
H(16)	14083	3470	9503	49
H(17)	15318	4178	10607	69
H(18)	1422	5112	11182	67
H(19)	11920	5350	10659	67
H(20)	10691	4650	9575	48
H(27)	7234(56)	2655(35)	7371(36)	45
H(28)	7349(63)	1363(38)	7514(39)	60
H(29)	9357(63)	715(39)	7430(40)	52
H(30)	11329(59)	1352(35)	7254(36)	50

* Equivalent isotropic U defined as one third of the trace of the orthogonalised U_{ij} tensor.

Table 10

Atomic coordinates ($\times 10^4$) and isotropic thermal parameters ($Å^2 \times 10^3$) for **11**

	x	*y*	*z*	*U*
Ru(11)	1170(1)	2003(1)	2420(1)	38(1)*
Ru(12)	−1132(1)	1328(1)	2238(1)	39(1)*
Ru(13)	−973(1)	2915(1)	1771(1)	35(1)*
Ru(14)	−919(1)	1664(1)	3618(1)	37(1)*
Ru(15)	−1411(1)	3365(1)	3309(1)	39(1)*
Ru(16)	985(1)	2726(1)	3658(1)	40(1)*
P(11)	−2250(1)	2313(1)	2793(1)	36(1)*
P(12)	520(1)	3302(1)	2531(1)	38(1)*
O(11)	2733(5)	538(3)	2949(3)	99(2)*
O(12)	3728(4)	2467(4)	1546(3)	110(3)*
O(13)	−633(5)	−397(3)	2804(3)	85(2)*
O(14)	−3530(5)	901(3)	1602(3)	79(2)*
O(15)	−3556(4)	3370(3)	1139(3)	91(2)*
O(16)	376(4)	4066(3)	585(2)	69(2)*
O(17)	−3231(5)	1068(3)	4640(3)	83(2)*
O(18)	630(5)	188(3)	4178(3)	88(2)*
O(19)	−4132(5)	3734(3)	3982(3)	88(2)*
O(110)	−1041(6)	5125(3)	3161(4)	116(3)*
O(111)	3245(5)	1628(4)	4111(3)	99(3)*
O(112)	2468(6)	4104(4)	3939(3)	98(3)*
C(11)	2079(6)	1077(4)	2782(4)	59(2)*
C(12)	2745(6)	2323(4)	1848(3)	61(2)*
C(13)	−802(6)	257(4)	2607(4)	57(2)*
C(12)	1931(6)	3585(4)	3826(3)	60(2)*
C(14)	−2638(6)	1046(3)	1860(4)	56(2)*
C(15)	−2558(6)	3190(4)	1367(3)	52(2)*
C(16)	−104(5)	3641(3)	1044(3)	45(2)*
C(17)	−2396(6)	1311(3)	4255(3)	51(2)*
C(18)	77(6)	745(4)	3946(3)	59(2)*
C(19)	−3175(5)	3556(4)	3716(3)	53(2)*
C(110)	−1167(6)	4461(4)	3213(4)	69(3)*
C(111)	2358(6)	2034(4)	3921(4)	63(2)*
C(120)	−733(7)	1825(4)	542(3)	60(2)*
C(121)	1(7)	1281(4)	208(4)	73(3)*
C(122)	1037(8)	851(5)	514(4)	86(3)*
C(123)	1369(7)	967(4)	1147(4)	73(3)*
C(124)	684(5)	1550(3)	1518(3)	46(2)*
C(125)	−364(6)	1982(3)	1209(3)	48(2)*
C(130)	−556(5)	2245(4)	4466(3)	47(2)*
C(131)	−776(5)	3066(3)	4321(3)	47(2)*
C(135)	−318(6)	1916(4)	5171(3)	61(2)*
C(132)	−774(6)	3546(4)	4870(4)	64(3)*
C(134)	−330(7)	2371(5)	5678(3)	71(3)*
C(133)	−557(7)	3194(5)	5525(3)	79(3)*
C(140)	1477(6)	4178(4)	2160(4)	58(2)*
C(150)	−4031(5)	2265(4)	2867(3)	53(2)*
Ru(21)	5681(1)	8246(1)	1898(1)	35(1)*
Ru(22)	4439(1)	7819(1)	3220(1)	35(1)*
Ru(23)	6846(1)	7108(1)	2940(1)	35(1)*
Ru(24)	3500(1)	7088(1)	2180(1)	35(1)*
Ru(25)	5667(1)	5949(1)	2033(1)	34(1)*
Ru(26)	5158(1)	7145(1)	977(1)	38(1)*
P(21)	4778(1)	6502(1)	3065(1)	34(1)*

Table 10 (continued)

	x	y	z	U
P(22)	6882(1)	7112(1)	1689(1)	35(1)*
O(21)	3883(5)	9603(3)	1339(3)	91(2)*
O(22)	8068(5)	9232(3)	1361(3)	88(2)*
O(23)	1995(5)	8875(3)	3114(3)	89(2)*
O(24)	3755(5)	7432(3)	4788(2)	77(2)*
O(25)	7366(6)	6105(4)	4318(3)	97(2)*
O(26)	9720(4)	7558(4)	2666(3)	92(2)*
O(27)	1344(5)	5965(3)	2793(3)	95(2)*
O(28)	1644(4)	8378(3)	1564(3)	89(2)*
O(29)	4646(5)	4319(2)	2645(3)	71(2)*
O(210)	7998(5)	5129(3)	1337(3)	94(2)*
O(211)	3985(6)	8527(3)	63(3)	107(3)*
O(212)	6992(5)	6738(4)	−242(3)	98(2)*
C(21)	4499(6)	9075(3)	1557(4)	56(2)*
C(22)	7190(6)	8868(3)	1550(3)	50(2)*
C(23)	2905(6)	8466(3)	3139(4)	57(2)*
C(24)	3999(6)	7578(3)	4201(3)	54(2)*
C(25)	7213(6)	6480(4)	3795(4)	61(2)*
C(26)	8660(5)	7362(4)	2753(3)	53(2)*
C(27)	2136(6)	6399(4)	2567(3)	55(2)*
C(28)	2368(5)	7919(4)	1816(4)	54(2)*
C(29)	5028(5)	4941(3)	2460(3)	45(2)*
C(210)	7114(5)	5420(3)	1612(3)	51(2)*
C(211)	4428(6)	8028(4)	418(4)	62(2)*
C(212)	6280(6)	6909(4)	196(3)	60(2)*
C(220)	6828(6)	8436(4)	3968(3)	54(2)*
C(221)	6599(7)	9201(4)	4064(4)	70(3)*
C(222)	5990(6)	9737(4)	3582(4)	62(2)*
C(223)	5644(5)	9535(3)	2965(4)	54(2)*
C(224)	5880(5)	8727(3)	2827(3)	43(2)*
C(225)	6455(5)	8180(3)	3333(3)	45(2)*
C(230)	3362(5)	6480(3)	1315(3)	43(2)*
C(231)	4392(5)	5919(3)	1249(3)	44(2)*
C(232)	4298(6)	5330(4)	820(3)	55(2)*
C(233)	3203(7)	5289(4)	481(3)	65(3)*
C(234)	2181(6)	5869(4)	531(3)	64(3)*
C(235)	2244(5)	6450(4)	922(3)	56(2)*
C(240)	8533(5)	7115(4)	1217(3)	55(2)*
C(250)	4201(6)	5776(3)	3810(3)	53(2)*

* Equivalent isotropic U defined as one-third of the trace of the orthogonalised U_{ij} tensor.

Acknowledgements

We are grateful to the SERC for the award of Research Studentships (to DAVM and SMN) and for support, the EEC through the framework of the Community Science Programme for support, the German National Scholarship Foundation (MW), and Johnson Matthey plc for a loan of ruthenium trichloride.

References

1 E.L. Muetterties, Pure Appl. Chem., 54 (1982) 83.
2 M.P. Gomez-Sal, B.F.G. Johnson, J. Lewis, P.R. Raithby and A.H. Wright, J. Chem. Soc., Chem. Commun., (1985) 1682.

3 M.D. Rausch, R.G. Gastinger, S.A. Gardner, R.K. Brown and J.S. Wood, J. Am. Chem. Soc., 99 (1977) 7870.
4 A.J. Deeming and M. Underhill, J. Chem. Soc., Dalton Trans., (1974) 1415.
5 R.J. Goudsmit, B.F.G. Johnson, J. Lewis, P.R. Raithby and M.J. Rosales, J. Chem. Soc., Dalton Trans., (1983) 2257.
6 M.A. Gallop, B.F.G. Johnson, J. Lewis, A. McCamley and R.N. Perutz, J. Chem. Soc., Chem. Commun., (1988) 1071.
7 M.I. Bruce, G. Shaw, and F.G.A. Stone, J. Chem. Soc., Dalton Trans., (1972) 2094.
8 M.I. Bruce, J.M. Guss, R. Mason, B.W. Skelton and A.H. White, J. Organomet. Chem., 251 (1983) 261.
9 C.W. Bradford, R.S. Nyholm, G.J. Gainsford, J.M. Guss, P.R. Ireland and R. Mason, J. Chem Soc., Chem. Commun., (1972) 87.
10 A.J. Deeming, R.E. Kember and M. Underhill, J. Chem. Soc., Dalton Trans., (1973) 2589.
11 A.J. Deeming, I.P. Rothwell, M.B. Hursthouse and J.D.J. Backer-Dirks, J. Chem. Soc., Dalton Trans., (1981) 1879.
12 S.C. Brown, J. Evans and L.E. Smart, J. Chem. Soc., Chem. Commun., (1980) 1021.
13 A.J. Deeming, S.E. Kabir, N.I. Powell, P.A. Bates and M.B. Hursthouse, J. Chem. Soc., Dalton Trans., (1987) 1529.
14 S.A.R. Knox, B.R. Lloyd, A.G. Orpen, J.M. Viñas and M. Weber, J. Chem. Soc., Chem. Commun., (1987) 1498.
15 N.M. Doherty, G. Hogarth, S.A.R. Knox, K.A. Macpherson, F. Melchior and A.G. Orpen, J. Chem. Soc., Chem. Commun., (1986) 540.
16 G.R. Doel, N.D. Feasey, S.A.R. Knox, A.G. Orpen and J. Webster, J. Chem. Soc., Chem. Commun., (1986) 542.
17 G. Hogarth, F. Kayser, S.A.R. Knox, D.A.V. Morton, A.G. Orpen and M.L. Turner, J. Chem. Soc., Chem. Commun., (1988) 358.
18 G. Hogarth, S.A.R. Knox, B.R. Lloyd, K.A. Macpherson, D.A.V. Morton and A.G. Orpen, J. Chem. Soc., Chem. Commun., (1988) 360.
19 N.J. Grist, G. Hogarth, S.A.R. Knox, B.R. Lloyd, D.A.V. Morton and A.G. Orpen, J. Chem. Soc., Chem. Commun., (1988) 673.
20 See ref. 4a of W.R. Cullen, S.T. Chacon, M.I. Bruce, F.W.B. Einstein and R.H. Jones, Organometallics, 7 (1988) 2273.
21 J.S. Field, R.J. Haines, and D.N. Smit, J. Chem. Soc., Dalton Trans., (1988) 1315.
22 S.A.R. Knox, D.A.V. Morton, A.G. Orpen and J.M. Viñas, to be published.
23 C.M. Friend and E.L. Muetterties, J. Am. Chem. Soc., 103 (1981) 773.
24 K. Natarajan, K. Zsolnai and G. Hüttner, J. Organomet. Chem., 209 (1981) 85.
25 A.J. Arce and A.J. Deeming, J. Chem. Soc., Dalton Trans., (1982) 1155.
26 H.J. Kneuper and J.R. Shapley, Organometallics, 6 (1987) 2455.
27 See H. van der Heijden, A.G. Orpen and P. Pasman, J. Chem. Soc., Chem. Commun., (1985) 1576, and references therein.
28 M.I. Bruce, J.G. Matissons and B.K. Nicholson, J. Organomet. Chem., 247 (1983) 321.
29 G.M. Sheldrick, SHELXTL, Göttingen, F.R.G., 1988.
30 International Tables for X-ray Crystallography, Vol. IV, Kynoch Press, Birmingham, 1974.